CENPD-292-NP

# BISON - One Dimensional Dynamic Analysis Code for Boiling Water Reactors: Supplement 1 to Code Description and Qualification

ABB Combustion Engineering Nuclear Operations

LEGAL NOTICE

THIS REPORT WAS PREPARED AS AN ACCOUNT OF WORK SPONSORED BY COMBUSTION ENGINEERING, INC. NEITHER COMBUSTION ENGINEERING, INC. NOR ANY PERSON ACTING ON ITS BEHALF:

A. MAKES ANY WARRANTY OR REPRESENTATION, EXPRESS OR IMPLIED INCLUDING THE WARRANTIES OF FITNESS FOR A PARTICULAR PURPOSE OR MERCHANTABILITY, WITH RESPECT TO THE ACCURACY, COMPLETENESS, OR USEFULNESS OF THE INFORMATION CONTAINED IN THIS REPORT, OR THAT THE USE OF ANY INFORMATION, APPARATUS, METHOD, OR PROCESS DISCLOSED IN THIS REPORT MAT NOT INFRINGE PRIVATELY OWNED RIGHTS; OR

B. ASSUMES ANY LIABILITIES WITH RESPECT TO THE USE OF, OR FOR DAMAGES RESULTING FROM THE USE OF, ANY INFORMATION, APPARATUS, METHOD OR PROCESS DISCLOSED IN THIS REPORT.

CENPD-292-NP

# BISON - One Dimensional Dynamic Analysis Code for Boiling Water Reactors: Supplement 1 to Code Description and Qualification

August 1994

ABB Combustion Engineering Nuclear Operations

TABLE OF CONTENTS





ABB

TABLE OF CONTENTS (Continued)

# 1 INTRODUCTION

The ABB transient analysis methods described in RPA-90-90-P-A (Reference 1) were approved for use in license applications by the U.S. NRC in 1989. RPA-90-90-P-A describes the BISON transient code and the code qualification for BWR transient analyses. The transient analysis design bases and overall reload methodology are summarized in the Reference Safety Report for BWR Reload Fuel (Reference 2). This Licensing Topical Report (LTR) supplements the approved transient analysis methods described in Reference 1 with features and options consistent with ABB reload applications world wide and intended future reload applications in the U.S. Specific features described and qualified allow (1) explicitly simulating single loop operations, (2) applications compatible with current fuel design codes and fuel design correlations (e.g., SVEA-96), and (3) improved modeling of BWR reactor components (i.e., steam line and separators).

The report is structured to complement and augment the original Licensing Topical Report, Reference 1. Section 2 provides summary and conclusions, including a cross reference of the contents of this Supplement Report to the original, approved Licensing Topical Report (Reference 1). Section 3 briefly reviews the transient analysis methods discussed in detail in Reference 1, Volume 1. Section 4 describes modifications to the BISON code. Section 5 describes the modifications to the application methodology of the BISON code for transient analysis, specifically input data and code options used. Section 6 provides qualification results in addition to those originally presented in Reference 1, justifying the changes discussed in Section 4 and 5.

# 2 SUMMARY AND CONCLUSIONS

## 2.1 Summary

This document provides changes to the ABB transient analysis methods for BWRs from the original description of methods and qualification described in the U.S. NRC approved Licensing Topical Report RPA-90-90-P-A (Reference 1). Tables 2-1, 2-2, and 2-3 summarize the code description, analysis inputs, and code qualification of the approved Licensing Topical Report. The tables also identify the sections of the original report being modified and a brief description of the modification presented in this document.

The modeling updates (discussed in Section 4) can be summarized as:

- The implementation of critical quality–boiling length formulations for a Critical Power Ratio correlation, such as the NRC approved XL-S96 CPR correlation for SVEA-96 fuel (Reference 3),
- Advanced steam line modeling enabling, for example, steam dynamic calculation in separate steam lines, steam bypass lines and steam cross flows between different steam lines,
- Individual recirculation loop dynamics enabling explicit simulation of Single Loop Operation (SLO), and
- Core boiling and condensation based on the Lellouche-Zolotar (EPRI) model, originally presented in Reference 1, which is a mechanistic, generic model with increased validity.

The application input changes (discussed in Section 5) can be summarized as:

- Fuel rod thermal data derived by the fuel performance code STAV6.2 (Reference 4) which shall be used in future applications and is under review by the NRC, and
- Geometric representation of the steam separator length over area (L/A) ratio rather than an effective L/A.

The additional qualifications presented (in Section 6) can be summarized as:

- Verification of the implementation of the XL-S96 correlation in BISON by comparison with CONDOR code steady state results and transient tests performed in the ABB FRIGG loop. This

implementation has been reviewed and accepted by the NRC in Reference 4. It is repeated in this document for completeness.

- Qualification of the advance steam line model by comparison to experimental and analytical results,

- Simulation of the three Peach Bottom 2 Turbine Trip events with the BISON modifications and refined description of boundary conditions for the events (i.e., scram timing, steam flow, and feedwater flow), and

- Sensitivity simulations of the Peach Bottom 2 Turbine Trip 1 with each new modifications introduced.

The critical power ratio qualifications reviewed and approved in Reference 3 and summarized herein, show that BISON conservatively predicts the dryout time and dryout onset during fast coolant flow decrease.

A steam line and turbine model was assessed by comparing numerical results with an analytical solution and experimental data. The model is particularly suited to predict steam flow and pressure transients in complex piping networks which include valves, tees, tanks, and turbine assemblies.

Comparisons to the Turbine Trip tests in the Peach Bottom 2 reactor at EOC2 conditions demonstrates the conservative prediction of neutron flux maximum which is important when determining the variation of critical power ratio during fuel licensing calculations.

## 2.2 Conclusions

The BISON code description and qualification presented in this document and in RPA-90-90-P-A (Reference 1) demonstrate that the BISON code and the hot channel model, SLAVE, are qualified for BWR transient analyses of BWR/2 through BWR/6. The general conclusions of the original NRC safety evaluation (Reference 9) are still valid. Based on the material presented in this supplement, several requirements of the original approval are confirmed and several requirements can be relaxed. These conclusions are summarized below.

(1) A NRC approved fuel performance code is used for fuel rod thermal data (i.e., fuel to cladding gap heat transfer). ABB intends to use the data based on the STAV6.2 code, currently under NRC review. An example application of STAV6.2

generated data is presented in the Peach Bottom 2 Turbine Trip simulations.

(2) The evaluations of critical power ratios are based on data and correlations approved by the NRC. In example, the NRC approved critical power ratio correlation for SVEA-96, XL-S96, is used for SVEA-96 fuel (Reference 3).

(3) The NRC requirement to justify the core flow imbalance as a result of the single, lumped recirculation loop representation is no longer applicable, since a two loop model has been introduced into BISON.

(4) The advanced steam line model eliminates the previous simplifying assumption of the steam line/turbine/bypass simulation. The advanced steam line model allows explicit modeling of multiple steam flow paths with comparable if not more accurate simulation results than the single steam line model described in Reference 1.

(5) For core channel boiling/condensation the Lellouche-Zolotar (EPRI) mechanistic model provides results which are comparable to the Solberg model over the range of applicability. Both models provide acceptable results.

(6) The requirement for justification of the slip and void correlation is still applicable when used for core pressure exceeding 9 MPa (1305 psia) while quality exceeds 40 percent or if the pressure exceeds 9.7 MPa (1405 psia).

(7) Comparisons and sensitivities may be made with the single (Method A) and multiple (Method B) fuel type methods for nuclear coefficients. The three-dimensional collapse (Method C) is the preferred approach for reload licensing evaluations.

(8) Justification will be provided when the recirculation pump model is used outside the first quadrants of the Karman-Knapp diagram or when in two-phase flow conditions.

(9) A NRC approved model shall be used when simulating control system functions for licensing basis applications.

**TABLE 2-1**

**BISON CODE DESCRIPTION MODIFICATIONS**

| Major Components | Description Status | Modification/Comment |
|---|---|---|
| Physical Model (Ref.1, Vol. 1, Chapter 2) | Unchanged from Reference 1 | -- |
| Thermal-Hydraulic Model (Ref.1, Vol. 1, Section 3) | Modified from Reference 1 with Options | Introduced Options for two jet pump drive loops (Section 4.2), and boiling length CPR correlation (Section 4.3). Use EPRI void model as base application option (Section 4.4). |
| Neutron Kinetic Model (Ref.1, Vol. 1, Section 4) | Unchanged from Reference 1 | -- |
| Fuel Heat Transfer Model (Ref.1, Vol. 1, Section 5) | Unchanged from Reference 1 | -- |
| Steam Lines Model (Ref.1, Vol. 1, Section 6) | Added to Reference 1, Volume 1, Section 6 | Introduced Option for advanced, multiple steam line model (Section 4.1) |
| General Time Integration Method (Ref.1, Vol. 1, Section 7) | Unchanged from Reference 1 | -- |
| System Models (Ref.1, Vol. 1, Section 8) | Unchanged from Reference 1 | -- |
| SLAVE Channel Model for Core or Coolant Channel (Ref.1, Vol. 1, Section 9) | Unchanged from Reference 1 | -- |
| Input Data Preparation (Ref.1, Vol. 1, Section 10) | Unchanged from Reference 1 | -- |
| Application of BISON (Ref.1, Vol. 1, Section 11) | Unchanged from Reference 1 | -- |
| Primary Variable Addresses on the General State Vector y (Ref.1, Vol. 1, App. A) | Unchanged from Reference 1 | -- |

**TABLE 2-2**

**TRANSIENT ANALYSIS INPUT MODIFICATIONS**

| Major Components | Description Status | Modification/Comment |
|---|---|---|
| BISON Peach Bottom Modeling Inputs (Ref.1, Vol. 2, Section 3.5) | Amended from Reference 1 cases incorporating new BISON modifications | Includes new fuel rod thermal data (Section 5.2), physical representation of separator L/A (Section 5.3), EPRI boiling model (Section 4.4), advanced steam line model (Section 4.1), and refined boundary conditions (Section 6.5.1.1). |
| TVO 1 BISON Modeling Inputs (Ref.1, Vol. 2, Section 4.3) | Unchanged from Reference 1 | -- |
| NRC Test Case Modeling Inputs (Ref.1, Vol. 2, Section 5) | Unchanged from Reference 1 | -- |
| Calculation of Neutron Kinetics Parameters (Ref.1, Vol. 2, Appx. A) | Unchanged from Reference 1, Volume 2, Appendix A | -- |
| Reload Licensing Modeling Inputs (Throughout Ref. 1) | Amended as discussed in this report | Includes new fuel rod thermal data, physical representation of separate L/A, EPRI void model, advanced steam line model. |

**TABLE 2-3**

**BISON CODE QUALIFICATION MODIFICATIONS**

| Major Components | Description Status | Modification/Comment |
|---|---|---|
| BISON models Separate Effects Qualification (Ref.1, Addendums 1, 2, 3, and 4) | Amended Reference 1 qualification base with evaluations for new BISON Models | Verification and validation of Advanced steam line model (Section 6.2 and 6.5.3.1), boiling length CPR correlation (Section 6.3), EPRI boiling model (Section 6.4 and 6.5.3.2), physical representation of separator L/A (Section 6.5.3.3), new fuel rod thermal data (Section 6.5.3.4). |
| BISON Qualification of Peach Bottom Turbine Trip Tests (Ref.1, Vol. 2, Section 3) | Amended from Reference 1 cases incorporating new BISON modifications | Peach Bottom Turbine Trip Tests including new fuel rod thermal data, physical representation of separator L/A, EPRI boiling model, advanced steam line model, and refined boundary conditions (Section 6.5.2). |
| TVO 1 Test 406 BISON/SLAVE Code Qualification (Ref.1, Vol. 2, Section 4) | Unchanged from Reference 1 | -- |
| NRC Test Case (Ref.1, Vol. 2, Section 5) | Unchanged from Reference 1 | -- |

# 3 OVERVIEW OF BISON CODE

BISON was developed by ABB Atom in 1971, based on the RAMONA-1 code. BISON is the ABB standard tool for BWR transient system response, transient fuel channel response, and is also used for stability analyses. The code has been used extensively for licensing of all ABB supplied fuel and reactors in Europe and the U.S.

The BISON code includes models for simulating a BWR reactor including the reactor core, recirculation loops, steam separators, feedwater, steam dome and steam lines, as well as a number of external (balance of plant) systems. BISON models the reactor coolant thermal-hydraulics, core neutron kinetics, fuel heat transfer, steam line pressure dynamics, and auxiliary plant systems.

A detailed description of the BISON code is provided in Reference 1 and with additional descriptions in Section 4 of this document. The following sections give a brief overview of the main code features.

## 3.1 Thermal-Hydraulic Models

BISON has a one-dimensional thermal-hydraulic model for the coolant loop of the reactor vessel, which can accommodate internal, external, and jet pumps. The coolant loop is divided into regions, which includes: downcomers, external recirculation loop, jet pumps, a core coolant and a bypass channel, risers and steam separators. These regions are further divided into subregions.

The conservation laws of mass and energy are solved for each node, for the general solution of a two-phase mixture in each of them. The integral momentum balance, on the other hand, is solved for the closed loops, or, optionally, through the core coolant channel, bypass channel and jet pump drive loop, respectively. Thermal non-equilibrium between the phases is modeled by assuming saturated vapor and employing an empirical correlation for mass transfer (boiling or condensation) between the phases. Different empirical slip correlations describe the unequal vapor and liquid velocities. The momentum balance utilizes empirical correlations for single and two-phase friction. Recirculation pumps are simulated by a homologous model. The hydrodynamic model can accommodate reversed flow and countercurrent flow.

## 3.2 Neutron Kinetics Models

A one-dimensional (axial finite difference) neutron kinetics model with two-group diffusion theory and up to six delayed neutron groups is used. The core is divided into the same subregions as in the thermal-hydraulic model. The core, as well as the top and bottom

reflector, may be subdivided into no more than 108 mesh points. Within each region the neutron kinetic parameters are kept constant and calculated from polynomials in the average moderator density, the moderator temperature, and the average fuel temperature of each subregion. Radially collapsed cross-section data are normally provided for 25 axial nodes in the core. A buckling term accounts for radial leakage. Control rods, rod motion, and rod insertion during scram are described, using a separate set of cross-sections, for the controlled cell.

The neutronic cross sections and their dependencies on coolant density, moderator temperature, fuel temperature and control rod density are either obtained directly from a 2D lattice code (e.g. the PHOENIX code) with boundary conditions from a 3D static core simulator (e.g. the POLCA code) for a single dominate fuel type (Method A), or several fuel types (Method B), or are derived using a 3D to 1D collapse technique from the original static 3D core simulator calculations (Method C). All three techniques are described in Appendix A of Reference 1, Volume 2.

### 3.3 Fuel Heat Transfer Models

The fuel thermodynamics represent a typical fuel rod with a radial one-dimensional finite difference model which solves the time dependent radial heat conduction in the fuel pellet, gap and cladding. The subdivision of the axial dimension is consistent with the hydrodynamic model. The source term is the sum of fission power (part of which is generated promptly in coolant and bypass channel) and decay power. The heat transfer from cladding to coolant is governed by empirical correlations, which depends on the flow regime.

### 3.4 Steam Line and Systems Model

BISON has options for a single steam line model and now also for an advanced, multiple steam line model (see Section 4.1). The single steam line model calculates the mass flow and pressure of all steam lines assuming isentropic behavior of the steam. Relief and safety valves and MSIVs can be located in the lumped steam line. The advanced multiple steam line model calculates the mass flow and pressure of each steam line modeled assuming isentropic behavior of the steam. With the multiple model, the turbine valves, bypass lines, and dump valves can be explicitly simulated allowing detailed steam line dynamic simulations.

There are detailed models for plant-specific control systems, steam line dynamics, feedwater system, safety and relief valves, the hydraulic scram rod insertion system, turbine, and generator. Most

of these models also may be substituted by assumed or given boundary conditions.

### 3.5 Solution Numerics

The steady-state solution for the coupled hydrodynamic, neutronic and fuel temperature models is obtained by power-void iterations, after which the initial state is calculated for the external system models.

### 3.6 BISON-SLAVE Single Channel Model

The BISON code actually consists of two versions, BISON-REACTOR which is used to model the global core response, and BISON-SLAVE which is used to model one channel in the core (normally the hot channel). A core channel model, BISON-SLAVE, is used for transient hot channel analysis, such as for transient critical power ratio (dryout margin) calculations. BISON-REACTOR and BISON-SLAVE are identical codes with BISON-SLAVE streamlined to include features required for core single channel applications.

In BISON-SLAVE the single fuel channel is assumed to have no influence on the rest of the core. Boundary conditions for the slave channel calculation are pressure, enthalpy and void content at core inlet and outlet, and fission power, which have been calculated in a preceding "average channel" BISON case.

# 4 BISON CODE MODIFICATIONS

The following model features have been introduced into the BISON code previously described in RPA-90-90-P-A (Reference 1):

- An advanced, multiple steam line model (Section 4.1),
- Two, explicit recirculation loops and jet pumps model (Section 4.2),
- A critical quality-boiling length formulation for the Critical power ratio (CPR) correlation (Section 4.3),

These features are options in the BISON code that do not alter the base structure or qualification of the code.

In addition, several slip and boiling/condensation models were described in Reference 1 for predicting the void content. For the fuel channel, the AA78 void correlation, in conjunction with the Solberg boiling/condensation model, was used and qualified for use in the original Licensing Topical Report. ABB has used the AA78 void correlation in conjunction with the Lellouche-Zolotar (EPRI) model extensively in applications in Europe, hence it is summarized (see Section 4.4) and qualified for U.S. applications in this document (see Section 6.4).

## 4.1 Advanced Steam Line Model (PARA)

The major objectives of the steam flow model, PARA, are to predict transients in an arbitrary steam line and turbine configuration. The model is a stand alone model that is incorporated in the BISON code.

The steam flow model is based on one-dimensional isentropic flow, including spatial acceleration and compressibility effects. In the finite difference form, the non-conservative form for momentum and energy equations is used. An implicit time integration scheme is used to eliminate a time-step limitation.

The main features of the model are:

- The ability to analyze single-phase flow steam transients in any piping network,
- Inclusion of models for valves, tees, turbine assembly,
- Interfaces to control systems,
- A consistent steady-state initialization technique,

- A restart facility,
- Time step algorithm for transient and steady-state solutions.

The model has been assessed by comparing numerical results with both analytical solution and experimental data (see Section 6.2).

### 4.1.1 Steam Balance and State Equations

A model of steam flow in a piping system must be conducted with a system of equations which describes the average flow and state of the steam within the flow channel. In the case of steam flow in simple channels, the average velocity, pressure, and enthalpy of steam across the channel is of interest. The system of equations which describes the average conditions within the channel is obtained from the local Navier-Stokes equations by use of averaging operations. Application of the averaging procedures will introduce, among other quantities, the shear stresses acting on the fluid by stationary surfaces bounding the flow field. These stresses are included in the model by use of empirical correlations for the friction factor.

The following simplifying assumptions have been selected to achieve computing efficiency:

- Gravity effects are negligible in the momentum and energy balance,
- Viscous dissipation is negligible in the momentum and energy balance,
- Pressure volume work is negligible in the momentum equation.

With these assumptions, the fluid balance equations of mass and momentum are as follows (Nomenclature is defined in Section 8):

- the mass conservation equation

$$A\frac{\partial \rho}{\partial t}+\frac{\partial W}{\partial z}=0, \tag{4.1-1}$$

- the momentum equation

$$\frac{1}{A}\frac{\partial W}{\partial t}+\frac{\partial}{\partial z}\left\{\frac{W^2}{\rho A^2}\right\}=-\frac{\partial P}{\partial z}-FW. \tag{4.1-2}$$

The conservation equations must be completed with the state equation to describe the steam density as a function of pressure and enthalpy:

$$\rho = \rho(P, h). \tag{4.1-3}$$

### 4.1.2 Numerical Scheme

The mass conservation (Equation 4.1-1) applied to cell $k$ in Figure 4-1 gives,

$$V_k \frac{\rho_k^{n+1} - \rho_k^n}{\Delta t} + W_{k+}^{n+1} - W_{k-}^{n+1} = 0. \tag{4.1-4}$$

A flow channel containing an abrupt area change is shown in Figure 4-1. Adding momentum equations over the left and the right half-volumes of the momentum cell $k+$ and applying the assumption of a steady-state incompressible flow about the vicinity of the interface $k+$, the following momentum equation is obtained,

$$I_{k+} \frac{W_{k+}^{n+1} - W_{k+}^n}{\Delta t} + 2\left\{\frac{W}{\rho}\right\}_{k+}^n \left\{\frac{W_{k+1}^{n+1}}{A_{k+1}^2} - \frac{W_k^{n+1}}{A_k^2}\right\} - \left\{\frac{W^2}{\rho^2}\right\}_{k+}^n \left\{\frac{\rho_{k+1}^{n+1}}{A_{k+1}^2} - \frac{\rho_k^{n+1}}{A_k^2}\right\}$$

$$= P_k^{n+1} - P_{k+1}^{n+1} + \frac{1}{2}\left\{\frac{W}{\rho}\right\}_{k+}^n \left\{\frac{1}{A_{k+1}^2} - \frac{1}{A_k^2}\right\} W_{k+}^{n+1} - F_{k+}^n W_{k+}^{n+1}, \tag{4.1-5}$$

where

$$I_{k+} = \frac{1}{2}\left\{\frac{L_k}{A_k} + \frac{L_{k+1}}{A_{k+1}}\right\}, \tag{4.1-6}$$

$$\rho_{k+}^n = \frac{1}{2}\left(\rho_k^n + \rho_{k+1}^n\right).$$

There are undefined unknowns $W_{k+1}^{n+1}$ and $W_k^{n+1}$ in equation (4.1-5). These variables can be expressed in terms of $W_k^{n+1}$ and the steam densities in cells $k$ and $k+1$ by setting up the continuity equations for the right and left half-volumes of the momentum cell. Substituting these variables into Equation 4.1-5 and rearranging the results, the mass flow rate can be expressed in terms of pressure and density of steam in the neighbor cells as follows,

$$W_{k+}^{n+1} = \frac{P_k^{n+1} - P_{k+1}^{n+1}}{d_{k+}} + a_{k+}\rho_{k+1}^{n+1} + b_{k+}\rho_k^{n+1} + c_{k+}, \tag{4.1-7}$$

where

$$d_{k+} = \left\{ \frac{I_{k+}}{\Delta t} + \frac{3}{2}\left(\frac{W}{\rho}\right)^{n}_{k+} \left\{ \frac{1}{A^2_{k+1}} - \frac{1}{A^2_k} \right\} + F_{k+} \right\}, \tag{4.1-8}$$

$$a_{k+} = \frac{1}{A^2_{k+1}} \left\{ \frac{W}{\rho} \right\}^{n}_{k+} \left\{ \frac{V_{k+1}}{\Delta t} + \left(\frac{W}{\rho}\right)^{n}_{k+} \right\} / d_{k+}, \tag{4.1-9}$$

$$b_{k+} = \frac{1}{A^2_k} \left\{ \frac{W}{\rho} \right\}^{n}_{k+} \left\{ \frac{V_k}{\Delta t} - \left(\frac{W}{\rho}\right)^{n}_{k+} \right\} / d_{k+}, \tag{4.1-10}$$

$$c_k = \left\{ -\frac{1}{\Delta t}\left(\frac{W}{\rho}\right)^{n}_{k+} \left\{ \frac{V_{k+1}}{A^2_{k+1}}\rho^{n}_{k+1} + \frac{V_k}{A^2_k}\rho^{n}_k \right\} + \frac{I_{k+}}{\Delta t} W^{n}_{k+} \right\} / d_{k+}. \tag{4.1-11}$$

The friction and local loss term has been expressed in a form of F·W in the momentum equation. The linear momentum balance requires models for the wall-to-fluid momentum exchange due to wall friction and local flow perturbations. Combining the friction term with the local loss term, the following is obtained:

$$F_{k+} = \left\{ \frac{1}{2}\left( \frac{L_k \lambda_k}{D_k} + \frac{L_{k+1}\lambda_{k+1}}{D_{k+1}} \right) + \zeta_{k+} \right\} \frac{|W_{k+}|}{2\rho_{k+}\underline{A}^2_{k+}} \tag{4.1-12}$$

where

$$\underline{A}_{k+} = \min\left\{ A_{k+1}, A_k \right\}.$$

The steam friction factor $\lambda$ is described by correlations for laminar and turbulent flow in smooth tubes as follows:

$$\lambda_{1k} = \frac{64}{\mathrm{Re}_k} \qquad \text{for } \mathrm{Re}_k < 1187$$

$$\lambda_{2k} = \frac{0.3164}{\sqrt[4]{\mathrm{Re}_k}} \qquad \text{for } \mathrm{Re}_k \geq 1187$$

where $\mathrm{Re}_k$ is the Reynold number in node $k$. To account for rough tubes, a minimum friction coefficient is applied,

$$\lambda_{3k} = \left\{ 2\log\left\{ D_k / 2\varepsilon_k \right\} + 1.74 \right\}^{-2}.$$

Finally, the friction factor λ for any flow conditions is found as,

$$\lambda_k = \max(\lambda_{1k}, \lambda_{2k}, \lambda_{3k}). \tag{4.1-13}$$

The Reynolds number is given by:

$$\mathrm{Re}_k = \frac{|W_{k+}|D_k}{\mu_k A_k} \tag{4.1-14}$$

The local momentum losses are modeled by use of the irreversible loss coefficients associated with the mechanical energy balance. These coefficients are functions of the geometric details of the flow channel and sometimes the flow direction. Momentum losses associated with flow through a sharp edged expansion or contraction are calculated according to the following:

for a sudden expansion:

$$\zeta = \left\{1 - \frac{A_1}{A_2}\right\}^2 \tag{4.1-15}$$

for a sudden contraction:

$$\zeta = 0.4\left(1 - \left\{\frac{A_2}{A_1}\right\}^2\right) \tag{4.1-16}$$

where $A_1$ and $A_2$ designate the cross section area of the channel before and after the restriction, respectively.

These momentum losses are added to the friction and local loss term, Equation 4.1-12. In addition local loss coefficients can be specified anywhere in the piping network.

Note that the pressure-loss term at any restriction is customary given in terms of the velocity at the smaller cross-section area.

### 4.1.3 Steam Properties

The steam properties are approximated by an isentropic model. The steam density and its derivative in pressure are computed from the following equations,

$$\rho = \rho(P) = \rho_0 \left\{\frac{P}{P_0}\right\}^{1/\kappa}, \tag{4.1-17}$$

$$\left\{\frac{\partial \rho}{\partial P}\right\} = \frac{1}{\kappa}\frac{\rho}{P}, \tag{4.1-18}$$

where $\rho_0$ and $P_0$ are initial steam density and pressure in the steam dome respectively.

### 4.1.4 Method of Solution

First, an assumption that the steam enthalpy is constant in the whole system and equal to the steam dome enthalpy. Substituting Equation 4.1-7 into the mass equation (Equation 4.1-4) the following is obtained:

$$-\frac{1}{d_{k+}}P_{k+1}^{j+1} + \left\{\frac{1}{d_{k+}} + \frac{1}{d_{k-}}\right\}P_k^{j+1} - \frac{1}{d_{k-}}P_{k-1}^{j+1} + \left\{\frac{V_k}{\Delta t} + b_{k+} - a_{k-}\right\}\rho_k^{j+1}$$

$$+a_{k+}\rho_{k+1}^{j+1} - b_{k-}\rho_{k-1}^{j+1} = \frac{V_k}{\Delta t}\rho_k^n + c_{k-} - c_{k+}. \tag{4.1.-19}$$

Now, $\rho_k^{j+1}$ is expanded in terms of $P$ and $h$ by the equation of state and the Newton-Raphson method as follows:

$$\rho_k^{j+1} = \rho_k^j + \left\{\frac{\partial \rho}{\partial P}\right\}_k^j \left\{P_k^{j+1} - P_k^j\right\} + \left\{\frac{\partial \rho}{\partial h}\right\}_k^j \left\{h_k^{j+1} - h_k^j\right\}. \tag{4.1-20}$$

Introducing the assumption $\left\{h_k^{j+1} - h_k^j\right\} = 0$ in Equation 4.1-20 and substituting Equation 4.1-20 into Equation 4.1-19 a linear system of equations in pressure will be obtained:

$$M \cdot P^{j+1} = D \tag{4.1-21}$$

where

$$M = M^n + M^j \quad \text{and} \quad D = D^n + D^j.$$

The set of Equation 4.1-21 is expressed in the matrix form. The coefficients with superscripts $n$ and $j$ are determined from the $n$-th time step values and from the $j$-th iteration step values, respectively. The set of equations (4.1-21) is solved iteratively, until a convergence criterion of the form

$$\left|\left(P^{j+1} - P^j\right) / P^{j+1}\right| < \varepsilon$$

is satisfied.

The next time step is performed after the mass flow rate and density have been determined from the momentum equation (Equation 4.1-7) and the equation of state (Equation 4.1-17).

### 4.1.5 Initial and Boundary Conditions

In order to solve a set of differential equations, initial and boundary conditions are required. From the viewpoint of the user, one of the most important features of the code is the ability to achieve a consistent solution of the steady-state equations. This solution determines the conditions throughout the system which are employed as initial conditions for the solution of the transient equations.

The steady-state capability is designed to provide the time-independent solution which may be of interest in its own right or as initial conditions for transient calculation. The steady-state solution can be found in a simple manner because of the good stability of the numerical scheme. Exactly the same equations are used in the steady-state solution as in the dynamic formulation.

Two types of fluid boundary conditions can be described in the model. These are steam state (i.e. steam enthalpy and pressure) and steam flow rate boundary conditions.

A steam state boundary condition allows specification of a known condition of the steam that exists outside of the system being modeled. For example, the steam dome can be defined as a boundary node with given steam pressure and enthalpy.

In the code, a flow boundary condition is indicated by designating the boundary node as a node with given flow rate. The steam mass flow rate is prescribed through input as a tabular function of time. The flow in a boundary node may be either positive (into the system) or negative (out of the system).

A branch node is designed to model a tee in the system. A vector momentum balance is considered in a tee. A completely rigorous model of a tee is not available, in the sense that the second-order diffusion terms in the Navier-Stokes equation have not been included, and all the geometric detail of a tee cannot be described. However, the momentum balance for the straight path and the momentum balance for the branch path are taking into account the turning of the flow from the straight to the branch path. In addition the local loss coefficient can be given by the user to account for loss of pressure in a tee junction. The pressure in branch nodes is computed in an iterative manner rather than in a direct solution of equation set (Equation 4.1-21). In other words instead of solving one matrix

equation for the whole system under consideration, Equation 4.1-21 is solved separately for each pipe, and then the pressure corrections for branch nodes are computed. The outer iterations are repeated until the mass flow error in the branch node is within a prescribed convergence criteria.

### 4.1.6 Component Models

The PARA steam line model includes models for flow control valves, safety/relief valves, and the turbine assembly.

#### 4.1.6.1 Valves

The code has models for simple flow control valves and safety/relief valves.

Simple flow control valves can be opened and closed by user-specified trips for opening and closing. Once the valve action occurs, the flow area for the valve is obtained from a specified area-versus-time table. Different area-versus-time tables can be provided for opening and closing of the valve. The flow area for the valve can also be supplied by a control system.

Safety/relief valves can be used to model steam flow from the system. The valves open and close on specified set pressures, delay times, and opening times. The steam flow rate is calculated based on a specified rated valve flow rate at a reference pressure.

#### 4.1.6.2 Turbine Assembly

The turbine assembly model requires a reasonable description of operating behavior of a turbine over a wide range of steam flow, inlet steam pressure, and some variation in speed. To meet these requirements the following assumptions have been adopted for the turbine assembly model:

(1) A quasi-static representation for a turbine assembly is adequate, that is a steady-state steam flow is considered and a simple first order time lag is introduced to modify the steam flow dynamics.

(2) Steam properties can be approximated by perfect gas laws.

(3) Turbine efficiency is known. In general, the value of turbine efficiency is well known at design operating conditions. It may also be available for some particular off-design conditions. A first approximation is to assume that the efficiency is constant for all conditions, and in the model in

question the user supplies the value of the constant stage efficiency.

(4) A turbine assembly can be considered equivalent to a series of orifices through which steam is passing, and between any two of which exists a box representing a bleeding point or a moisture separator-reheater.

For an isentropic steady-state process the steam flow through an orifice $k$ (Figure 4-2) can be expressed in terms of a pressure ratio $\Pi_k$ as,

$$W_k = \alpha_k \beta(\Pi_k) \frac{\sqrt{P_{k-1}}}{\sqrt{V_{k-1}}}, \tag{4.1-22}$$

where $\alpha$ is a constant proportional to the flow area and $\beta$ is a function of the pressure ratio $\Pi$.

For a given or guessed mass flow through the orifice, Equation 4.1-22 can be solved for $P_k$. If the inlet state point, outlet pressure, and turbine stage efficiency are known, then the outlet state point can be determined from the relationship:

$$h_k = h_{k-1} - \eta_k (h_{k-1} - h_{ks}). \tag{4.1-23}$$

The thermodynamic conditions at point $k$-$1$ will be known from the steam line model (if $k=1$) or from the solution of the thermal and hydraulic behavior for the previous orifice.

The turbine stage output $Q_k$ is defined by:

$$Q_k = W_k (h_{k-1} - h_k). \tag{4.1-24}$$

To complete the stage calculations the specific volume $v_k$ of steam at point $k$ has to be found. The revolution rate of the whole assembly is given by the following differential equation:

$$\frac{d\omega}{dt} = \frac{Q_t - Q_g / \eta_g}{I_t \omega}. \tag{4.1-25}$$

The moisture separator-reheater is treated as a single box in the turbine assembly model. The moisture separator-reheater removes the moisture from the inlet wet steam with efficiency defined by the user. The outlet cycle steam enthalpy is found from the steady-state steam mass and energy balance.

## 4.2 Parallel Jet Pump and Recirculation Pump Model

The BISON model described in Reference 1 includes models for simulating one lumped external recirculation pump loop, one lumped jet pump recirculation loop, or lumped internal recirculation pumps. A combined momentum balance is solved for the total recirculation flow through the downcomer, recirculation loops, and lower plenum as described in Volume 1, Section 3.7.5.3 of Reference 1. The jet pump component is modeled as described in Volume 1, Section 3.8.3.

In order to explicitly simulate asymmetric recirculation loop characteristics (i.e., single loop operation), a multiple loop model has been introduced into BISON. The multiple loop model can explicitly simulate the two jet pump recirculation loops and jet pumps of General Electric BWRs or several external recirculation loops of earlier BWR designs. For BISON to optionally simulate two parallel jet pump and recirculation pump loops, additional mass and momentum balance equations have been introduced into the code. This section describes the modified geometry and equations used to simulate multiple parallel recirculation loops.

### 4.2.1 Modified Code Geometry

The BISON code geometric representation of the BWR reactor is expanded to include pressures, flows, thermal properties and component models for two recirculation loops and jet pumps. Individual behavior of the two individual recirculation pumps is also explicitly modeled.

The system pressure control volume of the original, lumped jet pump recirculation loop model in BISON is shown in Figure 3.7.1B of Reference 1, Volume 1. Figures 4-3 and 4-4 show the direct extension of this model to two jet pump recirculation loops. Figure 4-3 shows the system pressure control volumes for two recirculation jet pump loops. Figure 4-4 shows the momentum balance using the θ-method time integration. The geometric representation of the jet pump and recirculation loop component is described in Section 3.8.3 and shown in Figure 3.8.3.1 of Reference 1, Volume 1. The recirculation pump model is described in Section 3.8.2 of Reference 1, Volume 1. The recirculation pump and jet pump component models are unaltered in the explicit two loop version. The momentum balances in the downcomer, jet pump and recirculation loops, however, are modified to include two parallel momentum balance for the two jet pumps and recirculation loops. This additional momentum balance introduces additional equations in the θ-method time integration matrix

solution. The next section presents the additional equations to be solved.

### 4.2.2 Modified Momentum Equations

The introduction of two parallel flow paths in the downcomer portion of the code requires new and modified momentum equations when implementing the two jet pump loop feature. The basic θ-method time integration approach used in BISON is described in Section 3.7.5 of Reference 1, Volume 1. The same solution and general equations are used with the two loop solution shown in Figure 4-4. The separate recirculation loop momentum balance described in Section 3.8.3 of Reference 1, now is part of the overall loop momentum solution. The actual equations solved are presented below.

To accommodate the two jet pumps, the momentum equation representing the downcomer/lower plenum flow path, illustrated in Figure 3.7.5.1 in Reference 1, Volume 1, is modified to represent six new flow paths as shown in Figure 4-4. The new flow paths are:

- Upper plenum to the jet pump suction plane [denoted d1]
- Recirculation loop 1 [denoted p(1)]
- Recirculation loop 2 [denoted p(2)]
- Jet pump number 1 throat inlet to tail exit [denoted j(1)]
- Jet pump number 2 throat inlet to tail exit [denoted j(2)]
- Jet pump exit to core inlet [denoted lp]

With these new flow paths the following junction flows are added to those defined in Section 3.7.5.2 in Reference 1, Volume 1:

$W_{i,d1}$ downcomer "1" inlet flow,

$W_{o,d1}$ downcomer "1" outlet (jet pump suction plane) flow,

$W_{i,p(i)}$ recirculation loop inlet flow for loop i,

$W_{o,p(i)}$ recirculation loop exit flow for loop i,

$W_{i,j(i)}$ jet pump inlet (suction and drive) flow for jet pump i,

$W_{o,j(i)}$ jet pump exit flow for jet pump i,

$W_{suc(i)}$ jet pump suction flow for jet pump i,

$W_{i,lp}$ lower plenum inlet flow,

$W_{o,lp}$ lower plenum outlet (core and bypass inlet) flow.

Note that the two explicit jet pump loops are denoted i = 1 and 2. Also the downcomer/lower plenum outlet flow $W_{od}$ in the original equations is now represented by the variable $W_{o,lp}$.

The downcomer/lower plenum equations presented in Section 3.7.5.3 of Reference 1, Volume 1 are modified for two parallel jet pump loops.

First the core inlet flow balance equation

$$W_{i1} + W_{i2} - W_{od} = 0 \qquad \text{(Matrix Equation 13)} \qquad (4.2\text{-}1)$$

is rewritten with the new lower plenum flow variable, $W_{o,lp}$

$$W_{i1} + W_{i2} - W_{o,lp} = 0 \qquad (4.2\text{-}2)$$

Next the downcomer/lower plenum composite momentum balance

$$a_{d11} W_{od} + a_{d12} B_d = C_{d1} \qquad \text{(Matrix Equation 14)} \qquad (4.2\text{-}3)$$

is decomposed into a set of mass and momentum equations for each recirculating jet pump loop (i = 1,2). Momentum balance for the downcomer "1" to the jet pump suction plane is:

$$a_{d1,11} W_{i,d1} + a_{d1,12} B_d + a_{d1,14} W_{o,d1} = C_{d1,1} \qquad (4.2\text{-}4)$$

and corresponding downcomer "1" control volume flow balance

$$W_{i,d1} - W_{o,d1} = Z_{o,d1} + Z_{i,d1} \qquad (4.2\text{-}5)$$

The mass balance at the downcomer "1" outlet is

$$W_{i,j(1)} + W_{i,j(2)} - W_{o,d1} = 0 \qquad (4.2\text{-}6)$$

and at each jet pump mixing plane is

$$W_{i,j(i)} - W_{i,p(i)} - W_{suc(i)} = 0 \qquad (4.2\text{-}7)$$

where (i) = (1) or (2). Momentum balance for the recirculation loop lines are:

$$a_{p(i)11} W_{o,p(i)} + a_{p(i),12} B_{p(i)} + a_{p(i),14} W_{o,p(i)} = C_{p(i),1} \qquad (4.2\text{-}8)$$

and corresponding recirculation line control volume flow balances are:

$$W_{i,p(i)} - W_{o,p(i)} = Z_{o,p(i)} + Z_{i,p(i)} \quad (4.2\text{-}9)$$

The recirculation line pressure gradient is:

$$B_{p(i)} - \frac{\rho_{f,d1}}{2}\frac{W^2_{o,d1}}{A^2_{d1}} + \frac{\rho_{f,suc(i)}}{2}\frac{W^2_{suc(i)}}{A^2_{suc(i)}})(1+L_{JP_i}) = 0 \quad (4.2\text{-}10)$$

Momentum balance for the jet pumps are:

$$a_{j(i),11}\, W_{i,j(i)} + a_{j(i),12}\, B_{j(i)} + a_{j(i),14}\, W_{o,j(i)} = C_{j(i),1} \quad (4.2\text{-}11)$$

and corresponding jet pump control volume flow balances are:

$$W_{i,j(i)} - W_{o,j(i)} = Z_{o,j(i)} \quad (4.2\text{-}12)$$

The jet pump pressure gradient is:

$$B_{j(i),L} - k_{j(i),L}\, W_{o,j(i)}\, |W_{o,j(i)}| = 0 \quad (4.2\text{-}13)$$

Finally, the lower plenum momentum balance is:

$$a_{lp,11}\, W_{i,lp} + a_{lp,12}\, B_{lp}\, a_{lp,14}\, W_{o,lp} = C_{lp} \quad (4.2\text{-}14)$$

and corresponding lower plenum control volume flow balance is:

$$W_{i,lp} - W_{o,lp} = Z_{o,lp} \quad (4.2\text{-}15)$$

and the flow balance at the lower plenum inlet from the jet pumps is:

$$W_{o,j(i)} + W_{o,j(2)} - W_{i,lp} = 0 \quad (4.2\text{-}16)$$

Next two Matrix equations are modified to be consistent with the above equations. The flow balance equation for the inlet to the core

$$-W_{od} - W_{11} + W_{B1} = 0 \qquad \text{(Matrix Equation 15)} \quad (4.2\text{-}17)$$

is rewritten using the new lower plenum variable $W_{o,lp}$

$$-W_{o,lp} - W_{11} + W_{B1} = 0 \quad (4.2\text{-}18)$$

Also in the closed flow path balance

$$-2k_1 |W_{i1}|^{n-1} W_{i1} + B_1 + B_R + B_d - 2k_{11} |W_{11}|^{n-1} W_{11}$$

$$= \Delta P_{up} - k_1 (|W_{i1}| W_{i1})^{n-1} - k_{11} (|W_{11}| W_{11})^{n-1}$$

$$\text{(Matrix Equation 2)} \quad (4.2\text{-}19)$$

the downcomer/lower plenum pressure difference $B_d$ is replaced by the sum of the individual components

$$B_d = B_{d1} + B_{p(1)} + B_{j(1)} + B_{jL(1)} + B_{lp} \tag{4.2-20}$$

yielding

$$-2k_1 |W_{i1}|^{n-1} W_{i1} + B_1 + B_R + B_{d1} + B_{p(1)} + B_{j(1)} + B_{jL(1)} + B_{lp}$$

$$-2k_{11} |W_{11}|^{n-1} W_{11} = \Delta P_{up} - k_1 (|W_{i1}| W_{i1})^{n-1} - k_{11} (|W_{11}| W_{11})^{n-1} \tag{4.2-21}$$

The local pressures at the jet pump mixing plane, $P_{mix(i)}$, is defined as described in Section 3.8.3 of Reference 1, Volume 1. Rewritten for each jet pump, (i) = (1), (2), using the above defined nomenclature, yields:

$$P_{mix(i)} = P_{d1} + dP_{asi(i)} + dP_{suci(i)} \tag{4.2-22}$$

where the suction flow entrance acceleration pressure drop (reversible) of jet pump (i), $dP_{asi(i)}$, is calculated as

$$dP_{asi(i)} = \left(\rho_{f,d1} \frac{W_{o,d1}}{A^2_{d1}} + \rho_{f,suc} + \frac{W^2_{suc(i)}}{A^2_{suc(i)}}\right) \tag{4.2-23}$$

and the suction flow entrance irreversible pressure drop of jet pump (i), $dP_{suc(i)}$, is calculated as:

$$dP_{suci(i)} = \frac{L_{JPi(i)}}{2} \rho_{f,suc} \frac{W_{suc(i)}^2}{A^2_{suc(i)}} \tag{4.2-24}$$

The recirculation loop (i) pressure gradient $B_{p(i)}$, is calculated as

$$B_{p(i)} = P_{mix(i)} - P_{d1} = \frac{1}{2}\rho_{f,d1} \frac{W^2_{o,d1}}{A^2_{d1}} - \frac{1}{2}\rho_{f,suc(i)} \frac{W^2_{suc(i)}}{A^2_{suc(i)}} + \frac{1}{2} L_{JPi(i)} \rho_{f,suc(i)} \frac{W^2_{suc(i)}}{A^2_{suc(i)}} \tag{4.2-25}$$

This equation corresponds to Equation 4.2-10 above.

In the set of equations presented above the definitions of the flow path coefficients are the same as those presented in Section 3.7.5.1 of Reference 1, Volume 1. Specifically:

$$a_{k,11} = Z_{3,k} + \theta h\, \theta_f \frac{d(\Delta P_{f,k})}{d<W>_k}, \quad (4.2\text{-}26)$$

$$a_{k,12} = -\theta h, \quad (4.2\text{-}27)$$

$$a_{k,14} = \theta h\, (1-\theta) \frac{d(\Delta P_{f,k})}{d<W>_k}, \quad (4.2\text{-}28)$$

$$C_{k,1} = \theta h\, ( \Delta P_{e,k} - \Delta P_{f,k} ) + \frac{d(\Delta P_{f,k})}{d<W>_k} ( \theta_f W_{i,k}^{n-1} + ( 1-\theta_f ) W_{o,k}^{n-1} ) ) + A_{o,k} - Z_{2,k}, \quad (4.2\text{-}29)$$

$$A_{o,k} = I_k^{n-1} + ( 1-\theta )\, h\, ( B_k - \Delta P_k )^{n-1}, \quad (4.2\text{-}30)$$

$$B_k = P_k - P_{k+1}, \quad (4.2\text{-}31)$$

and the terms $Z_{2,k}$ and $Z_{3,k}$ are defined in Section 3.7.2 of Reference 1, Volume 1. In Equations 4.2-26 through 4.2-31 the subscript k identifies the (consecutive) loop section (e.g., d1, j, p, lp, etc.) and $P_k$ stands for the loop section reference pressure at the loop section inlet.

Equations 4.2-5 through 4.2-16 are introduced into the θ-integration model along with the modified Equations 4.2-2, 4.2-4, and 4.2-21. The numerical solution technique used in BISON to solve the complete set of equations is unchanged, as described in Section 3.7.5.2 of Reference 1, Volume 1. With the introduction of the jet pump drive loop momentum balance into the θ-integration model as described above, the momentum balance equation for the drive loop described in Section 3.8.3 of Reference 1, Volume 1 is no longer used. The remaining discussion of the jet pump given in Section 3.8.3 is still applicable with the equations solved individually for each one of the jet pump loops, using appropriate inlet and outlet properties as identified in Figure 4-4.

## 4.3 Implementation of Boiling Length CPR Correlation

The critical quality–boiling length formulation for calculating the specific fuel design critical power ratios (CPR) has been implemented into BISON. The NRC approved Licensing Topical Report UR-89-210-P-A (Reference 3) describes in detail the critical quality–boiling length formulation including the correlation for SVEA-96 fuel, named XL-S96. UR-89-201-P-A also describes the implementation of

the XL-S96 correlation in the CONDOR steady state thermal hydraulic code (Reference 5) and in the BISON transient analysis code. The implementation of the XL-S96 correlation into BISON is qualified in UR-89-210-P-A against transient dryout test loop data. In Section 6.3 of this report, the steady state verification against CONDOR results and the transients test qualification results of UR-89-210-P-A are presented for completeness. This implementation has been previously reviewed and approved by the NRC in UR-89-201-P-A.

## 4.4 The EPRI Boiling and Condensation Model

In order to describe core dynamics for bounding BWR operational transients, the core thermal-hydraulic model selection is essential. Of primary importance are the boiling/condensation model and the slip correlation (void) model. These models can greatly influence the code ability to predict the core average and a hot channel transient response. In Section 3.4.3 and 3.4.4 of Reference 1, Volume 1, two alternative models for the boiling mechanism are described, the Solberg's and the Lellouche-Zolotar's (EPRI) models, respectively. The Solberg's model includes three constants determined through benchmarking. The EPRI mechanistic model prescribes all constants.

In Reference 1, Volume 2 the code qualification simulations for U.S. licensing applications were performed using the Solberg's model with specified calibration constants. The calibration constants were determined such that the BISON axial coolant density matched the POLCA three dimensional nodal simulator (Reference 10) calculated average axial density. Specifically, in the qualifications the constants were determined for the three different conditions of the Peach Bottom tests.

The EPRI boiling/condensation model as described in detail in Section 3.4.4 has been qualified and used extensively in European applications and is intended to be used in future U.S. licensing applications.

In the EPRI model the heating process is considered as being made up of two physical parts: surface heating and condensation and direct bulk heating and condensation. In addition to heating processes, vapor is generated by temporal and spatial pressure changes. Hence, vapor generation is considered to be a result of three sources:

(1) Vapor formed at the wall due to wall superheating,

(2) Bulk boiling due to direct deposition of energy (through neutron thermalization and gamma attenuation), and

(3) Flashing and condensation due to transient and spatial pressure effects.

[Proprietary Information Deleted]

Requalification of BISON with the EPRI boiling/condensation model is presented in Section 6.5.3.2.

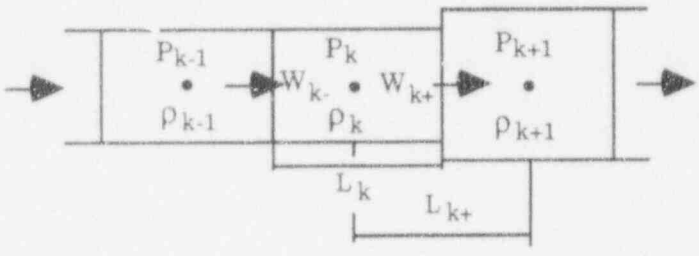


Figure 4-1 Steam line Model Computational Cell

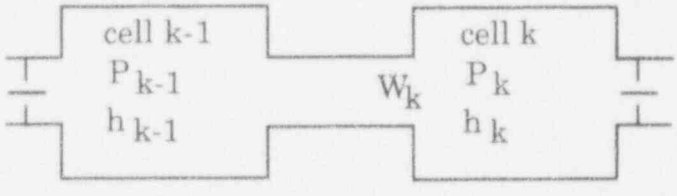


Figure 4-2 A Turbine Stage Model

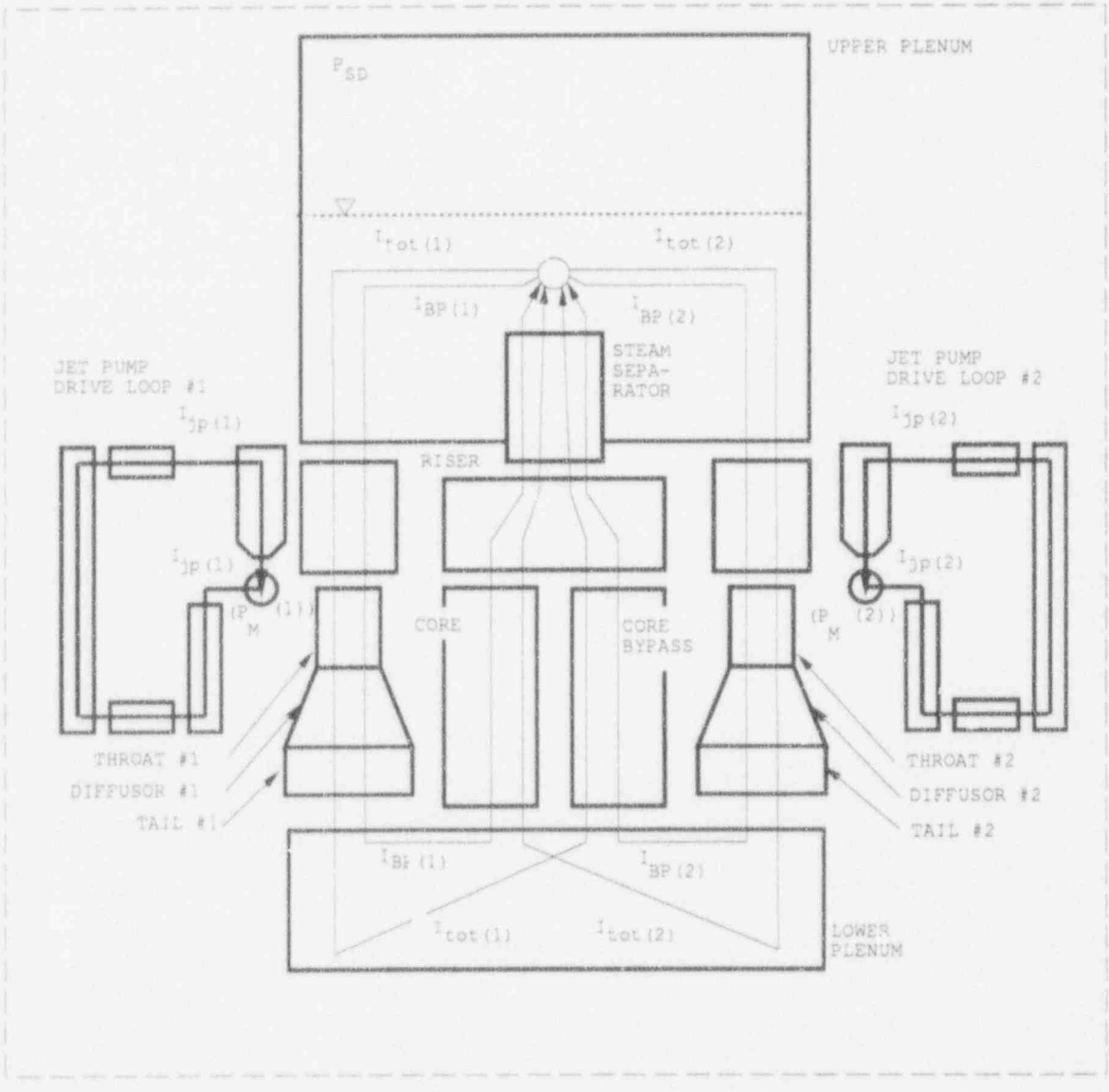


Figure 4-3 Control Volume for System Pressure with Two Jet Pump Recirculation Loops

2 Bypass Channel Inlet Flows
2 Jet Pumps
2 Jet Pump Loops

47 Equations

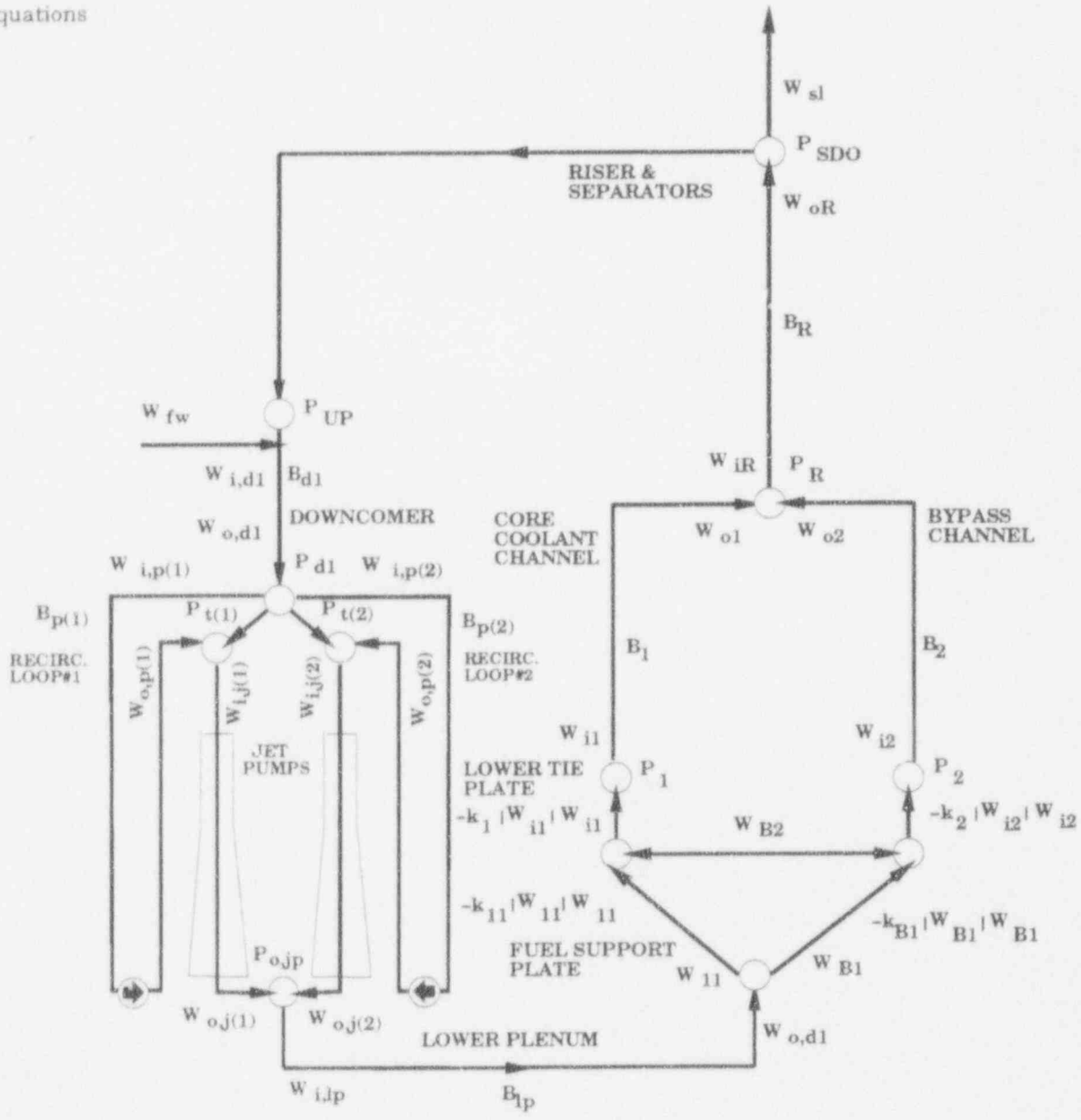


Figure 4-4 θ - Method Time Integration for the RPV with Two Jet Pump Recirculation Loops

# 5 TRANSIENT ANALYSIS INPUT MODIFICATIONS

The BISON computer code has numerous input options available for different code applications. In the BISON Licensing Topical Report RPA-90-90-P-A (Reference 1) most of the input options are described. Also in Reference 1, the options used in the presented code qualification and to be used in U.S. licensing application are identified. The key BISON code model and input options used in the cases presented in Reference 1 and in the additional qualification cases of this report are summarized in Section 5.1. Modifications to the BISON model options used have been discussed in Section 4 above. Modifications to the BISON input options are discussed in Section 5.2 and 5.3 below.

## 5.1 Key Transient Analysis Inputs

The key BISON model and input options to be used for licensing applications as identified in Reference 1 are summarized in Table 5-1. Table 5-1 also shows the model and input options recommended to be used in licensing applications as a result of the modifications described in this supplemental report. Of the changes (shown in bold), the steam line, boiling/condensation, and recirculation loop model changes are described in Section 4. The fuel rod thermal data and steam separator geometry inputs are discussed below. Additional qualification simulations addressing all these changes are presented in Section 6.

## 5.2 Fuel Rod Thermal Data from the STAV6.2 Code

During transients which occur over a time period of seconds, the time constants of the fuel rods are important. The generated energy is conducted through the uranium fuel pellet, across the gas gap, and through the fuel rod cladding. The rod is prepressurized with a gas, (e.g. helium) with a relatively high heat transfer conductance. During the fission processes fission gases with lower heat transfer conductance are generated which is mixed both with the uranium pellet (gas cavities) and with the existing gas. Depending on the pellet crack-up assumptions, pellet and cladding surface roughness, and equivalent gas gap heat transfer coefficient, a corresponding equivalent pellet-fission gas conductivity can be established.

ABB has developed a code which simulates the pellet and gas gap properties during expected or extreme core conditions. The current version of the fuel performance code is STAV6.2 described thoroughly in Reference 4. A short description is given below.

The STAV6.2 code affords a best-estimate analytical tool for predicting steady-state fuel performance for operation of light water

reactor fuel rods including $Gd_2O_3$-$UO_2$ fuel. STAV6.2 calculates the variation with time of all significant fuel rod performance quantities including fuel and cladding temperatures, fuel densification, fuel swelling, fission product gas release, rod pressure, gas gap conductance, cladding stresses and strains due to elastic, thermal, creep and plastic deformations, rod growth, cladding oxidation and cladding hydriding. Other submodels include burnup dependent radial power distribution for both $UO_2$ and $Gd_2O_3$-$UO_2$ fuel, fuel grain growth and helium release.

The STAV6.2 code captures the following phenomena which determines properties important for typical fast transient analysis:

- Accelerated fission gas release at high power bursts during substantial periods of time (and a decreased gas gap heat transfer coefficient), and
- Momentary increase of power leading to pellet volume expansion and corresponding gas gap decrease (and an increased gas gap heat transfer coefficient).

The input to the BISON code is derived based on realistic or conservative power histories. An equivalent gas gap heat transfer coefficient is formulated as a function of fuel pellet average temperature. [Proprietary Information Deleted]

## 5.3 Modification to L/A Relations for the Steam Separators

The one-phase liquid and the gaseous phase in the steam separators are described by complex flow paths because of the separating effect of the vanes and the rotating liquid above the vanes (Figure 5-1). As discussed in Sections 3.7.3 and 3.8.1 of Reference 1, Volume 1, it was anticipated that the flow behavior with regard to impulse and mass transport could be described by a model that describes the rotating liquid flow as an increased L/A ratio. Qualification sensitivity studies (See Section 6.5.3.3) show, however, that the conservatism is significant. Other sources of conservatism also have been identified, e.g. a high isentropic exponent in the steam line model. However, eliminating uncertainties in the steam line modeling in several qualification cases by using measured steam dome pressure, still yielded conservative results. Therefore the simulation conservatism is attributed to the separator model. [ Proprietary Information Deleted ] Hence the length to area parameter (L/A) specified for the BISON steam separator model will be, in future applications, based on measured geometric distances.

TABLE 5-1

MODEL AND INPUT OPTIONS FOR LICENSING APPLICATIONS

PROPRIETARY INFORMATION DELETED

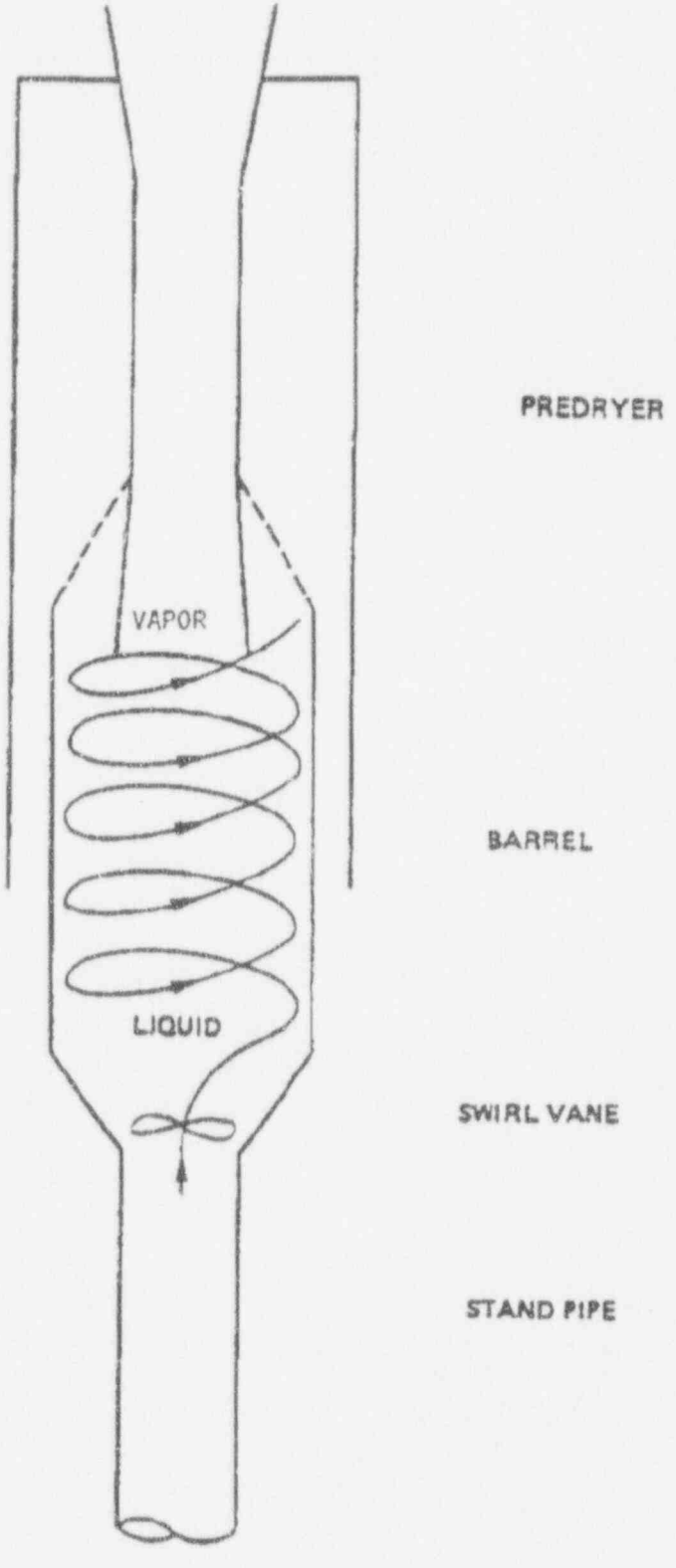


Figure 5-1 Schematic of a Steam Separator

# 6 QUALIFICATION OF MODIFICATIONS

This section presents additional qualification of the BISON code for U.S. reload licensing transient analyses. The Licensing Topical Report RPA-90-90-P-A (Reference 1, Volume 2) presents the qualification bases justifying the use of BISON and BISON-SLAVE for U.S. reload licensing transient analyses. The following sections summarize the complete BISON qualification base and present additional qualification cases to support the model and input modifications described previously in Sections 4 and 5.

## 6.1 BISON Qualification Bases

The BISON and BISON-SLAVE code qualification bases include extensive comparisons with analytical solutions, integral loop tests, and reactor plant tests. In particular, transient dryout predictions have been verified against ATLAS (ABB Atom/General Electric), FIX (Studsvik), and FRIGG (ABB Atom) test loop data, using appropriate CPR correlations. System and core responses in pressurization transients have been verified against Peach Bottom 2 turbine trip tests, and against similar tests and operational transients in ABB built reactors (i.e., the inadvertent pressurization transient at TVO I).

In addition, core stability prediction in a jet pump reactor has been verified against Peach Bottom 2 stability tests and in internal pump reactors (ABWR design), and against ABB Atom natural circulation test data. Such tests have been performed in the internal pump reactors Forsmark 1, TVO I and II, and Oskarshamn 3.

## 6.2 Advanced Steam Line Model Qualification

The advanced steam line and turbine model (PARA) has been verified and validated by comparison of calculations with analytical solutions and experimental data.

The PARA steam line model was compared to analytical solutions presented in BNL-NUREG-51186 (Reference 8). Reference 8 presents analytical solutions assuming both viscous and inviscid flow, as shown in Figure 6-1. The assumed conditions for comparing the computed results obtained from the steam line model for viscous and inviscid flow and the analytical solutions are given in Table 6-1.

The initial conditions for the simulation assume that the steam line is in steady-state. The transient simulation assumes a constant steam dome pressure and that the turbine stop valve closes in 0.1 seconds.

The numerical solutions obtained from the PARA steam line model are shown in Figure 6-2. The code was executed with imposition of laminar and isentropic steam flow. It can be seen from comparison of Figure 6-1 and 6-2 that the steam line model calculates correctly the pressure amplitude at the turbine stop valve.

The new steam line model (PARA) is also compared to the original model (described in Reference 1, Volume 1, Section 6) for the first Peach Bottom 2 Turbine Trip test (TT1). The result of the comparison yield less than 2 percent deviation in maximum APRM. The results are discussed in detail in Section 6.5.3.1.

## 6.3 Critical Quality-Boiling Length Formulation Verification

The implementation of critical quality-boiling length form of the correlation for calculation of the critical power ratio has been verified and validated against other codes and test loop data. The correlation for SVEA-96 fuel (XL-S96) and its implementation in BISON has been reviewed and approved in Reference 3. For completeness the qualification is summarized below.

### 6.3.1 BISON Comparison with Static Thermal-Hydraulic Code CONDOR

In order to verify the implementation of the CPR correlation in the transient analysis code BISON, a comparison was made with the static thermal hydraulic code CONDOR (Reference 5). The comparison was performed for four different steady state points, shown in Table 6-2. As also shown in Table 6-2, the deviations in calculated critical power ratio (CPR) using the XL-S96 correlation, between CONDOR and BISON are [ Proprietary Information Deleted].

### 6.3.2 BISON Comparison with FRIGG Transient CPR Tests

The BISON calculations of the FRIGG transient CPR tests have been presented in detail in Section 7 of Reference 3. The results of the comparisons are briefly summarized here for completeness.

Five transient cases were selected for the evaluation. All five cases have the same general transient appearance as shown schematically in Figure 6-3. The initial test conditions (power and mass flow), and delay between the start of the flow coast down and the start of the power reduction were varied. These data, as well as the power and flow conditions at the start of the transient are summarized in Table 6-3. The system pressure was approximately 7 MPa and the inlet subcooling maintained at 10°C in all five cases. Dryout was detected in cases 1395, 1435, 1437 and 1440. No indication of dryout was detected in case number 1394.

Experimental boundary conditions were used as input to the BISON model. The resulting transient variation of CPR (calculated using the XL-S96 correlation) is summarized in Table 6-4. [ Proprietary Information Deleted ]

## 6.4 BISON Void Model Qualification

In order to qualify the resulting static thermal-hydraulic performance of the selected boiling and void correlations in the BISON code, comparisons are made with measured average void in the FRIGG loop. A comparison of the AA78 slip correlation and Solberg boiling correlations was shown in Amendment 2, Response 22 in Reference 1. A comparable comparison has been performed with the AA78 slip correlation and EPRI boiling correlations.

In the FRIGG loop, measurements of voids were performed for test series OF64A and OF64B (References 6 and 7). The test section consisted of a 64-rod configuration. The void measurements were done utilizing collimated gamma rays and detectors. Ten axial positions and 12 collimated rays at each axial location were used. The recorded signals were processed through a mathematical algorithm in order to derive average coolant densities. A set of calibrations were done at varying conditions in order to secure the density derivation.

The comparison between BISON calculations and FRIGG measurements is done for average densities at different axial locations. For the total comparison, the Root Mean Square (RMS) and the bias is evaluated.

[ Proprietary Information Deleted ]

## 6.5 BISON Reactor Transient Qualification

The basis for code qualification given in Reference 1, Volume 2 included three Peach Bottom 2 turbine trip tests, one TVO I pump trip test and a simulation of the NRC reference case. The qualification base and sensitivity cases presented in Reference 1 are summarized for convenience in Table 6-6 through 6-9. The tables show the key model and input options used in base and sensitivity cases and the resultant maximum calculated and measured APRM (in % of rated power). More details of all these cases are given in Reference 1, Volume 2.

Additional qualification cases were run in support of the modifications presented in this report. The three Peach Bottom 2 tests were chosen for the new calculations, because pressurization

transients represent the limiting event for most U.S. BWRs. These tests also have been accepted as the industry standard for boiling water reactor transients. The new evaluation includes STAV6.2 generated fuel thermal data, the EPRI boiling/condensation model, the advanced steam line model, and revised L/A for the steam separators.

### 6.5.1 Peach Bottom 2 Turbine Trip Tests Description

The Peach Bottom 2 turbine trip tests are described in detail in Section 3 of Reference 1, Volume 2. The three turbine test results are summarized in Table 6-10.

#### 6.5.1.1 Refined Boundary Conditions

The BISON model and boundary conditions are also described in Section 3 of Reference 1. Several refinements have been made of the boundary conditions used in the original Peach Bottom 2 simulations based on more detailed evaluations of the event data. The revised boundary conditions are the delay between the APRM setpoint and start of control rod insertion ("scram delay") and the steam and feedwater flow boundary conditions.

The delay time between APRM setpoint and start of control rod insertion has been revised based on the plant data taking into account:

- Measurement errors in the APRM registration (based on measured LPRM registrations),
- Delay between scram setpoint (APRM) and APRM relay closure,
- Delay between APRM closure and control rod movement.

The original and revised individual total delays between scram setpoint and start of control rod insertions used in the turbine trip simulations are shown in Table 6-11.

Refined boundary conditions were used in the revised simulations of the three Peach Bottom 2 turbine trip events based on reevaluations of the plant data. Figures 6-5 to 6-7 show comparison of the original and revised flow boundary conditions.

The BISON calculations presented in Reference 1, Volume 2, were also done using different assumptions concerning input preparation for neutronic cross sections. In Reference 1 the methods used included radial collapse of neutronic cross sections with static 3D

perturbation calculations in order to derive cross section dependencies (Method C), and two types of calculations using weighted averaged BISON polynomial expressions derived directly from the 2D neutronic lattice code (Method A and B). The generation of neutronic input in this report was done using a more detailed implementation of Method B. Specifically:

(1) Fuel type specific neutronic cross section and parametric dependencies were derived for different void histories.

(2) Average nuclear dependencies were derived for each axial node. Two sets of data, with and without control rods, were derived.

(3) The final axial cross section dependencies were calculated based on the average axial control rod density.

This approach differs from the original calculations in Appendix A of Reference 1, Volume 2, in that a refined 2D lattice calculation was performed and no void coefficient correction was introduced.

#### 6.5.1.2 Peach Bottom 2 Turbine Trip 1 with Refined Boundary Conditions

The Peach Bottom 2 turbine trip 1 simulation presented in Reference 1 was repeated with the refined boundary conditions. The key inputs for the two cases are summarized in Table 6-13. The transient comparison to the test data is presented in Figure 6-8(a), (b), and (c).

[ Proprietary Information Deleted ]

### 6.5.2 Additional Qualification with Modifications

The Peach Bottom 2 turbine trip tests were simulated with the BISON code including the refined test boundary conditions and new model and input features presented in this report.

#### 6.5.2.1 New BISON Inputs for Modifications

The model and input modifications introduced in the Peach Bottom 2 BISON model are:

- The PARA steam line model with geometric data consistent with the original PIPE model,
- Switch the boiling correlation used from the Solberg to EPRI model,

- Use the geometric dimensions of the separators in determining the inertia length divided by area (L/A) term,
- Use gas gap heat transfer coefficients generated from STAV6.2 code.

Details of generating the gas gap heat transfer coefficients is discussed below.

The Peach Bottom 2 core contains 764 fuel bundles. At the End of Cycle 2 (EOC2) tests, the core consisted of a number of General Electric (GE) fuel designs. GE 7x7 inserted during reactor start-up and reload fuel of GE 8x8 with various fractions of gadolinia and uranium enrichment. Table 6-12 presents the various fuel bundles.

The core consisted of 75 percent 7x7 and 25 percent 8x8 fuel. [Proprietary Information Deleted]

### 6.5.2.2 Peach Bottom Turbine Trip Tests with BISON Modifications

The three Peach Bottom 2 turbine trip tests (TT1, TT2, and TT3) were simulated with BISON using the refined boundary conditions and BISON model modifications. The key input parameter for the cases relative to those presented in Reference 1 are summarized in Table 6-14. The maximum APRM from the simulations presented in this report, Reference 1, and the test are:

| **Case** | **APRMmax (%) (Figure Number)** | | |
|---|---|---|---|
| | **Revised** | **Original (Ref. 1, Vol. 2)** | **Measured** |
| TT1 | [ Proprietary Information Deleted ] (Figure 6-12) | 327 (Fig. 3.5 and 3.6) | 230 |
| TT2 | [Proprietary Information Deleted ] (Figure 6-13) | 373 (Fig. 3.7 and 3.8) | 278 |
| TT3 | [Proprietary Information Deleted ] (Figure 6-14) | 334 (Fig. 3.9 and 3.10) | 332 |

Detailed simulation/test comparisons are shown in Figures 6-12 through 6-15.

[ Proprietary Information Deleted ]

### 6.5.3 Sensitivity Study of Model and Input Modifications

To further understand the impact of the modifications introduced in BISON, simulations of the Peach Bottom 2 TT1 event were performed for each new modification. Specifically, starting with the refined boundary conditions simulation (Case 18), each modification was introduced and compared to the previous case:

- Introducing the new steam line model (Case 22),
- Replacing the Solberg model with the EPRI subcooled boiling model (Case 23),
- Using the geometrical L/A ratio for the steam separators (Case 24),
- Replacing the PAD generated thermal fuel data with STAV6.2 generated data (Case 19),

The key inputs for the cases are summarized in Table 6-15 along with the resultant maximum APRM.

#### 6.5.3.1 Evaluation of Advanced Steam Line Model

The comparison of the TT1 test case with the "old" and "new" steam line model (Case 18 versus 22) is shown in Figures 6-15(a) and (b). The "new" model inputs were the same as for the "old" model, i.e. one average steam line with three main sections. The steam flow boundary condition is prescribed at the turbine/bypass tee in both cases. [ Proprietary Information Deleted ]

#### 6.5.3.2 Evaluation of EPRI Boiling/Condensation Model

The new qualification cases included the EPRI subcooled boiling model. Starting with the BISON model from Case 22, the EPRI subcooled boiling model was introduced (Case 23). [ Proprietary Information Deleted ]

#### 6.5.3.3 Evaluation of Geometric L/A for the Steam Separators

The impact of modeling the geometric L/A ratio for the steam separators instead of an effective L/A which includes delay and momentum of the cylindrical one-phase liquid flow path above the

separator vanes is evaluated in this section. The TT1 simulation, Case 23, was changed to model the geometric separator L/A (Case 24). Comparison between the geometric and effective L/A cases is shown in Figure 6-16(a) and (b). [ Proprietary Information Deleted ]

| Parameter | Geometric L/A | Effective L/A | Measured |
|---|---|---|---|
| APRMmax (%) | [ Proprietary Information Deleted ] | [ Proprietary Information Deleted ] | 230 |
| Δvoid decrease (-) | [ Proprietary Information Deleted ] | [ Proprietary Information Deleted ] | - |

[ Proprietary Information Deleted ]

#### 6.5.3.4 Evaluation of STAV6.2 Fuel Rod Thermal Data

The BISON TT1 simulation Case 24 can now be compared to the final qualification simulation (Case 19) to assess the impact of the STAV6.2 generated fuel rod performance data. [ Proprietary Information Deleted ]

[ Proprietary Information Deleted ]

TABLE 6-1

STEAM LINE QUALIFICATION CASE CONDITIONS

| Parameter | Value |
|---|---|
| Pipe cross section area | 0.1542 $m^2$ |
| Pipe length | 65.99 m |
| Number of cells | 40 |
| Initial mass flow rate | 268.3 kg/s |
| Initial density | 35.738 $kg/m^3$ |
| Pressure in steam dome | 6.88 MPa |

TABLE 6-2

STEADY STATE COMPARISON BETWEEN BISON AND CONDOR PREDICTION OF CRITICAL POWER RATIO (CPR)

PROPRIETARY INFORMATION DELETED

TABLE 6-3

INITIAL AND FINAL EXPERIMENTAL BOUNDARY CONDITIONS IN TRANSIENT CPR TESTS

PROPRIETARY INFORMATION DELETED

TABLE 6-4

BISON-SLAVE DRYOUT PREDICTION FOR SVEA-96 TRANSIENT CPR TESTS

PROPRIETARY INFORMATION DELETED

TABLE 6-5

BISON-SLAVE DRYOUT TIME PREDICTION
FOR SVEA-96 TRANSIENT CPR TESTS

PROPRIETARY INFORMATION DELETED

TABLE 6-6

PEACH BOTTOM 2 TURBINE TRIP 1
SIMULATION CASES IN REFERENCE 1

PROPRIETARY INFORMATION DELETED

TABLE 6-7

PEACH BOTTOM 2 TURBINE TRIP 2
SIMULATION CASES IN REFERENCE 1

PROPRIETARY INFORMATION DELETED

TABLE 6-8

PEACH BOTTOM 2 TURBINE TRIP 3
SIMULATION CASES IN REFERENCE 1

PROPRIETARY INFORMATION DELETED

TABLE 6-9

TVO-I AND NRC SIMULATION CASES IN REFERENCE 1

PROPRIETARY INFORMATION DELETED

**TABLE 6-10**

**DEFINITION OF PB2 TURBINE TRIP TESTS AND MEASURED MAXIMUM POWER**

| Test | Reactor Power (MW/%) | Core Flow Rate (kg/s) | Peak Core Average Power (% of rated) |
|---|---|---|---|
| TT1 | 1562/47.4 | 12,764 | 230 |
| TT2 | 2030/61.6 | 10,332 | 278 |
| TT3 | 2275/69.1 | 12,839 | 332 |

**TABLE 6-11**

**TOTAL SCRAM DELAY TIMES FOR PEACH BOTTOM 2 TURBINE TRIP SIMULATIONS**

| PB2 Test Case | TT1 | TT2 | TT3 |
|---|---|---|---|
| Original Scram Delay (s) | 0.180 | 0.180 | 0.180 |
| Revised Scram Delay (s) | [ Proprietary Information Deleted ] | [ Proprietary Information Deleted ] | [ Proprietary Information Deleted ] |

TABLE 6-12

FUEL TYPES P' ESENT DURING THE PEACH BOTTOM 2, EOC2 TESTS.

| Type | Number of fuel rods | Number of $Gd_2O_3$ rods | $Gd_2O_3$ enrichment (%) | $U^{235}$ enrichment (%) |
|---|---|---|---|---|
| 2 | 7x7 | 4 | 3 | 2.50 |
| 3 | 7x7 | 3 + 2 | 3 and 4 | 2.50 |
| 4 | 8x8 | 5 | 3 | 2.74 |
| 5 | 8x8 | 5 | 2 | 2.74 |
| 6 | 8x8 | 5 | 2 | 2.60 |

TABLE 6-13

PEACH BOTTOM 2 TURBINE TRIP 1
WITH REVISED BOUNDARY CONDITIONS

PROPRIETARY INFORMATION DELETED

TABLE 6-14

PEACH BOTTOM 2 TURBINE TRIP
SIMULATIONS WITH MODIFICATIONS

PROPRIETARY INFORMATION DELETED

TABLE 6-15

PEACH BOTTOM 2 TURBINE TRIP 1
SENSITIVITY TO MODIFICATIONS

PROPRIETARY INFORMATION DELETED

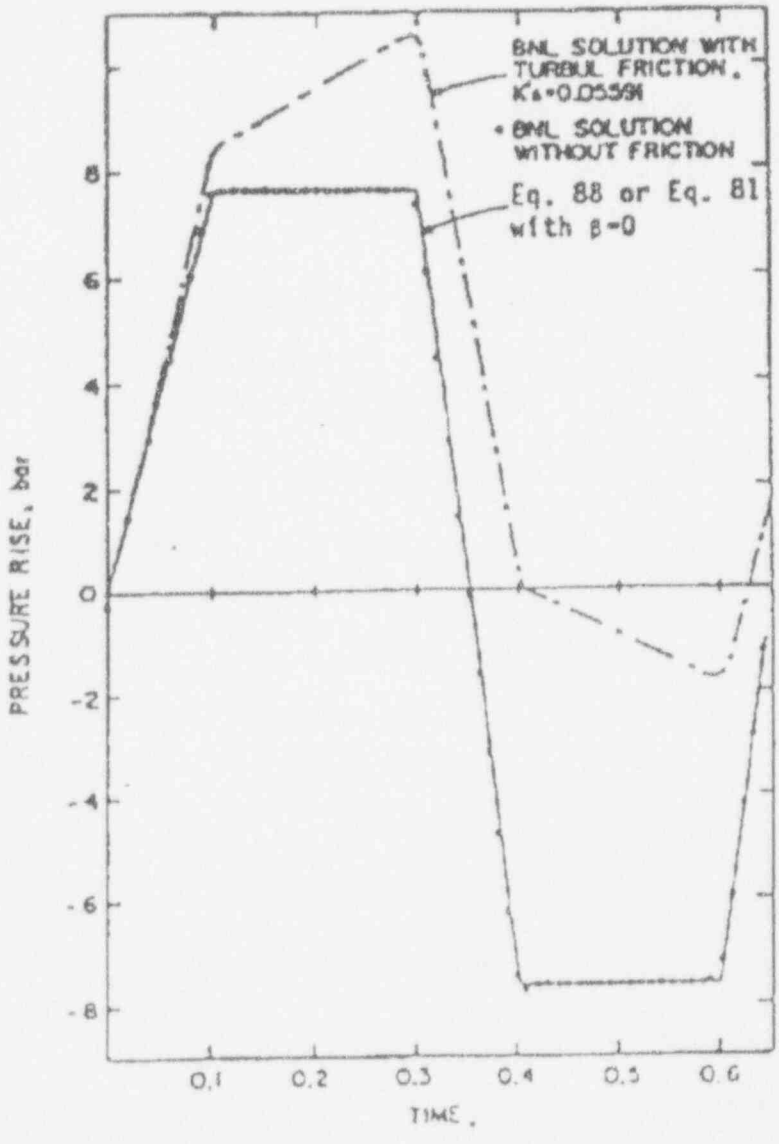


Figure 6-1 Viscous and Inviscid Analytical Steam Line Pressure Solutions (from Reference 8)

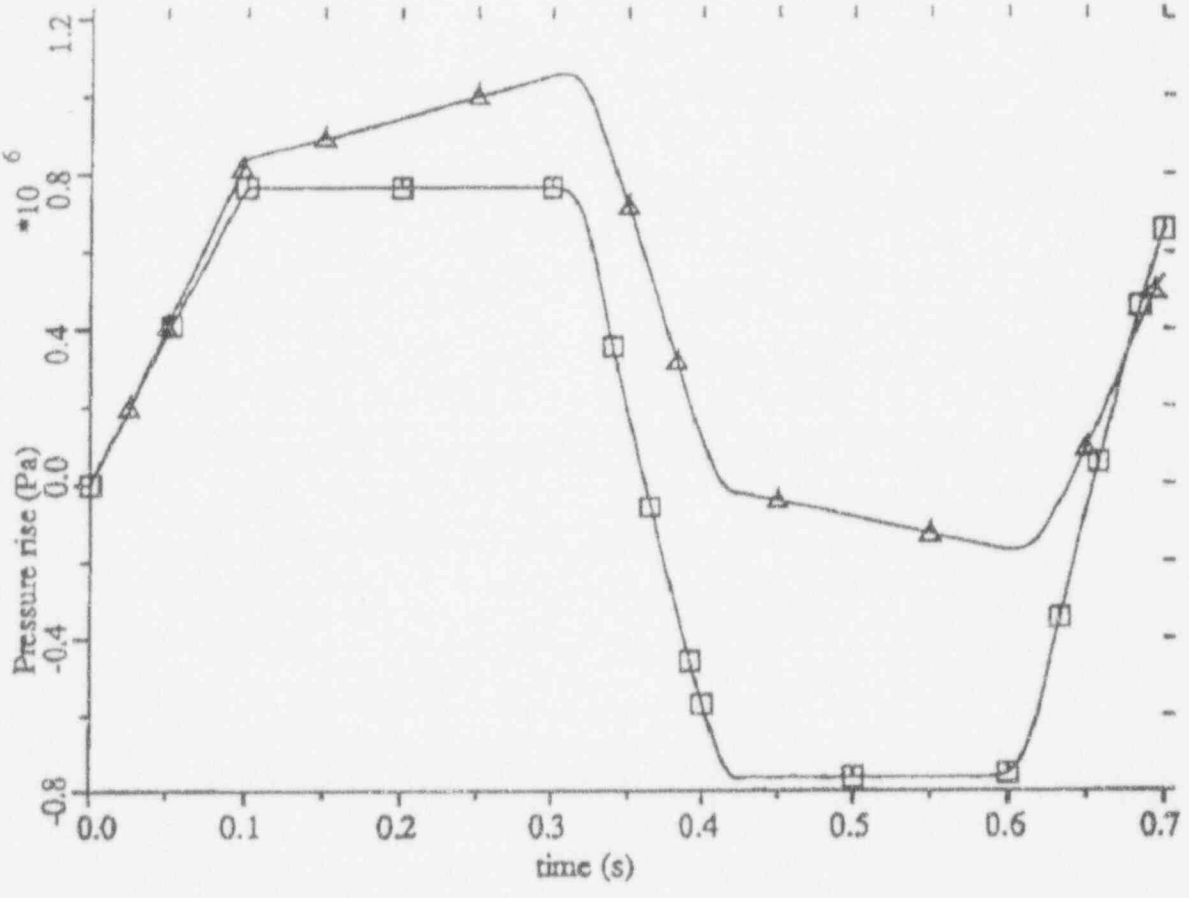


Figure 6-2 BISON PARA Steam Line Model Predictions of Analytical Solutions from Reference 8

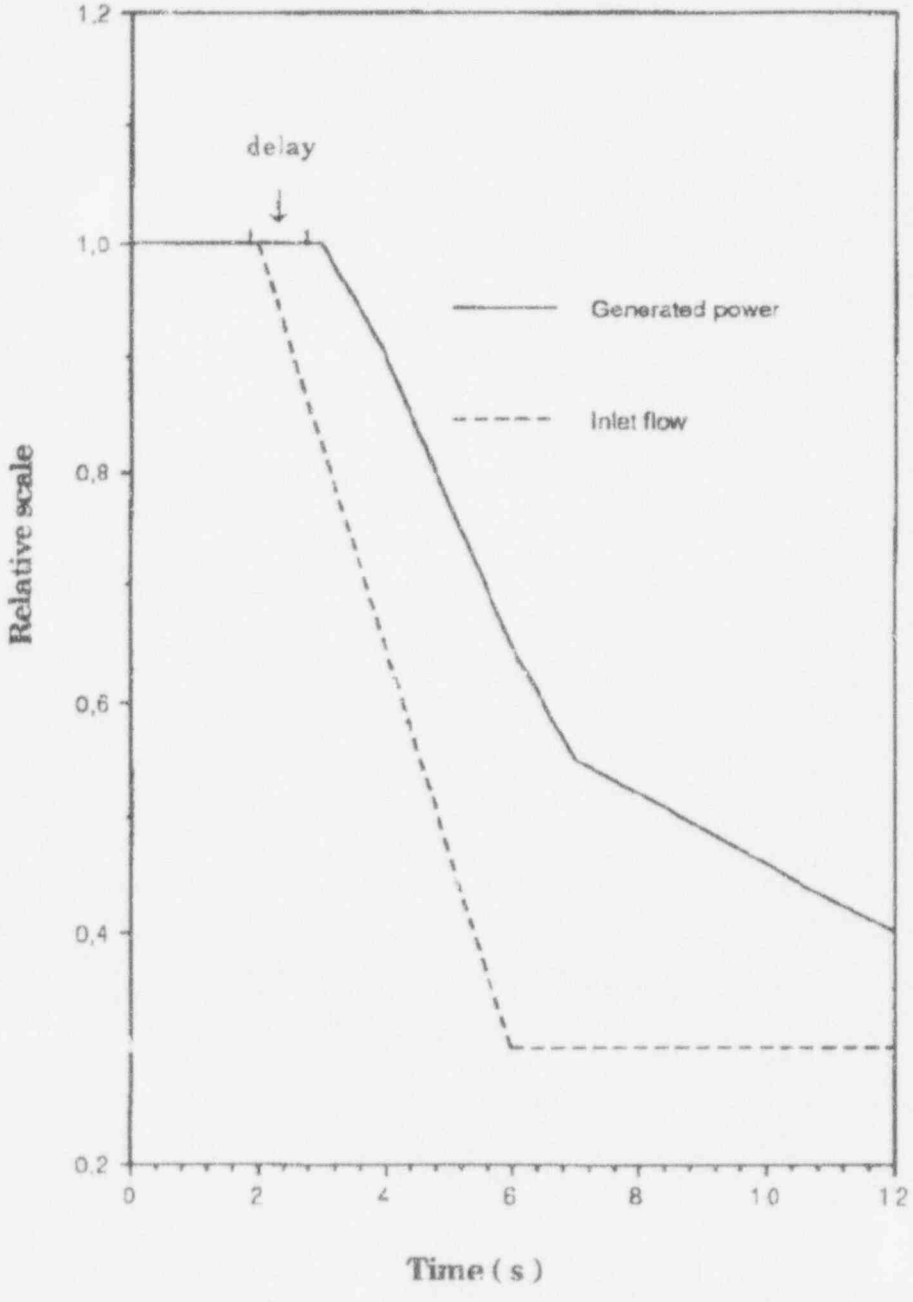


Figure 6-3 Schematic of FRIGG Transient CPR Test Conditions

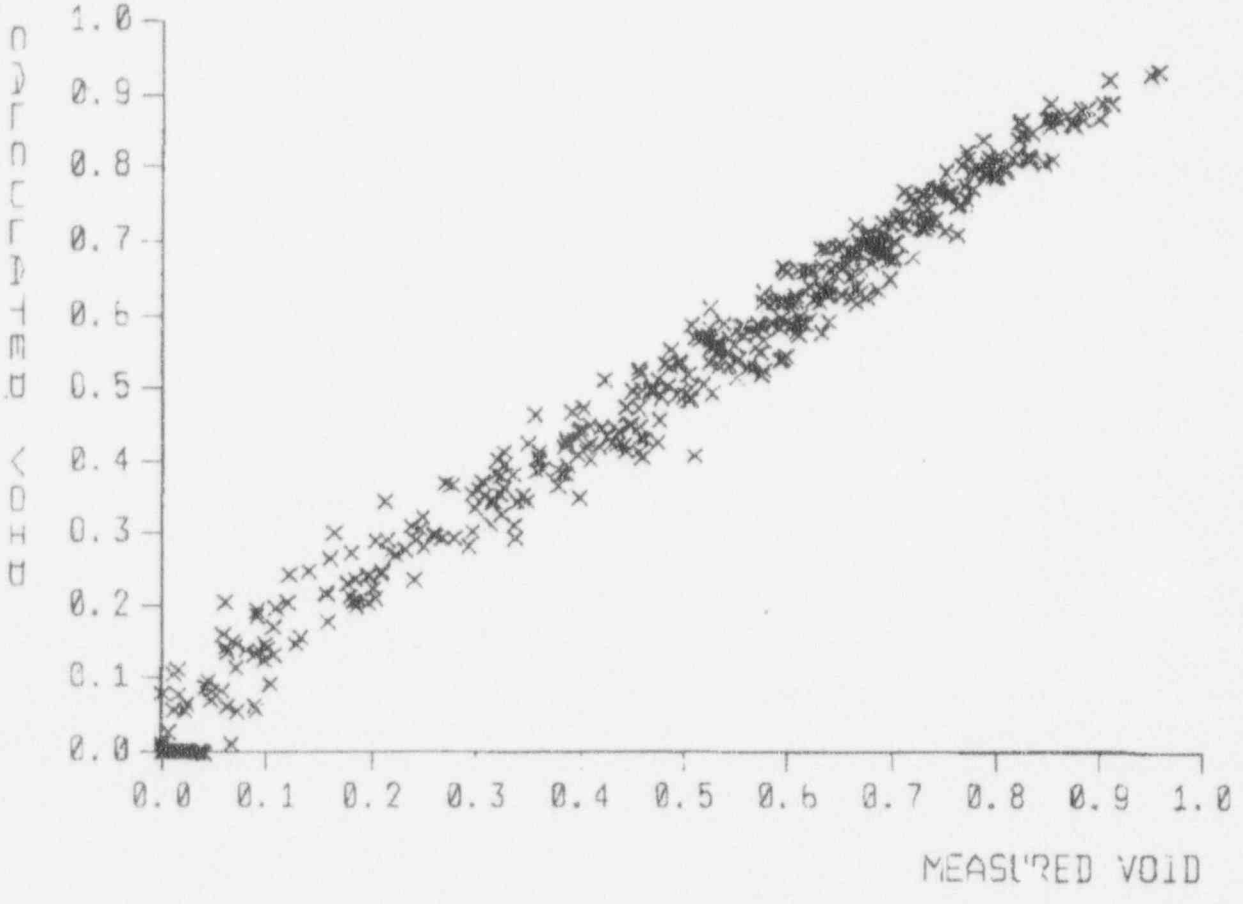


[[ Proprietary Information Deleted]

Figure 6-4 Comparison of BISON Calculated Void with Measured Void in the FRIGG-64 Loop

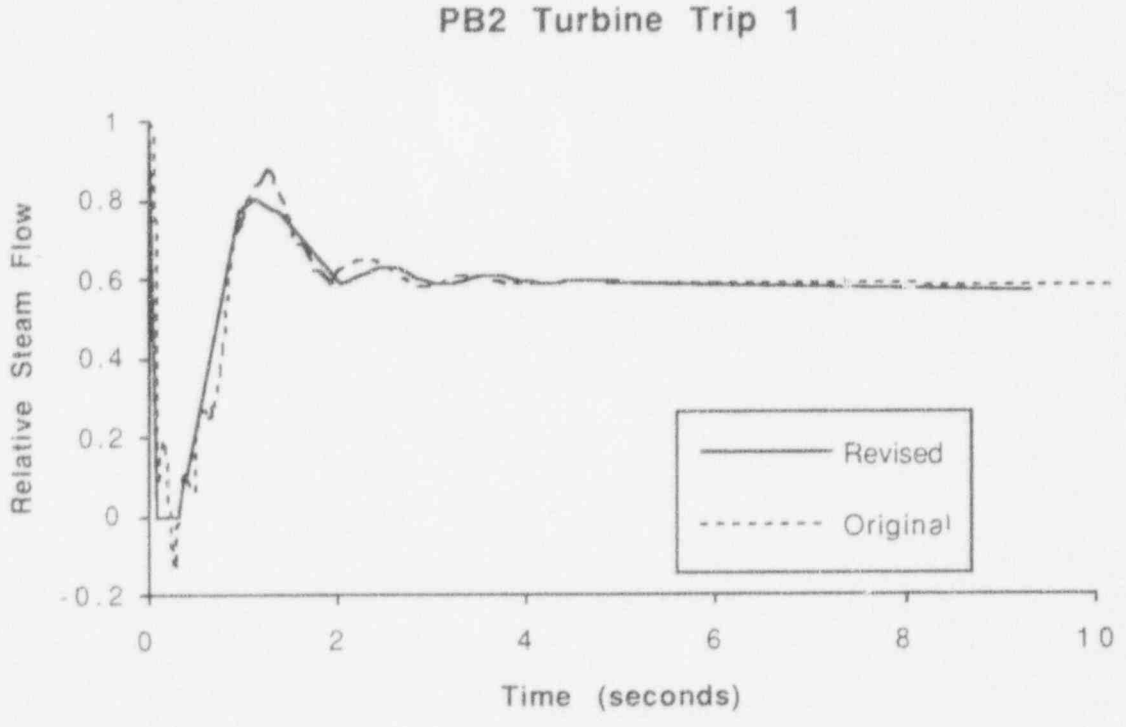


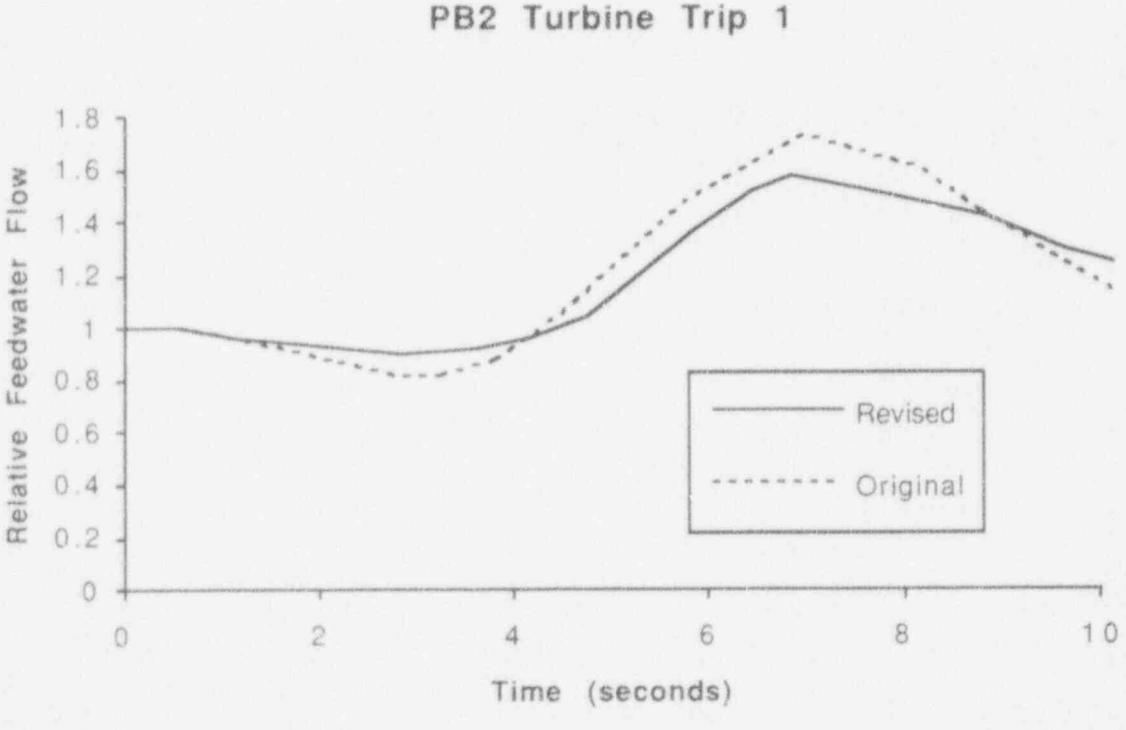


Figure 6-5 Comparison of Peach Bottom 2 TT1 Boundary Conditions

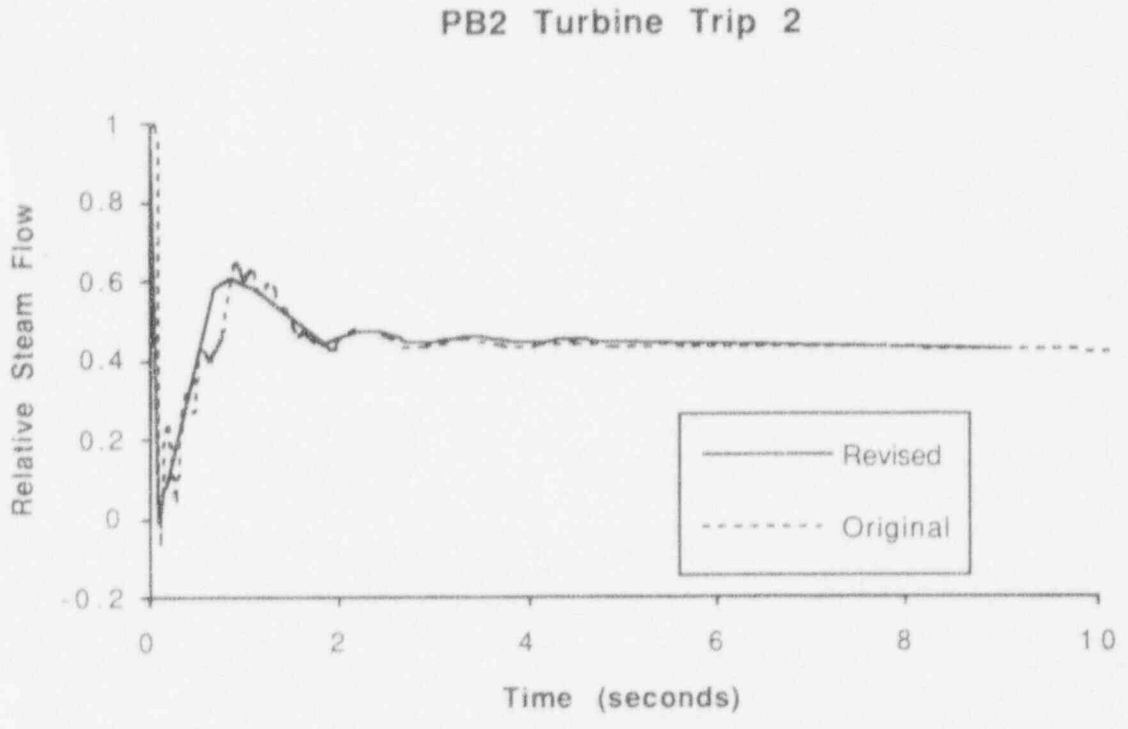


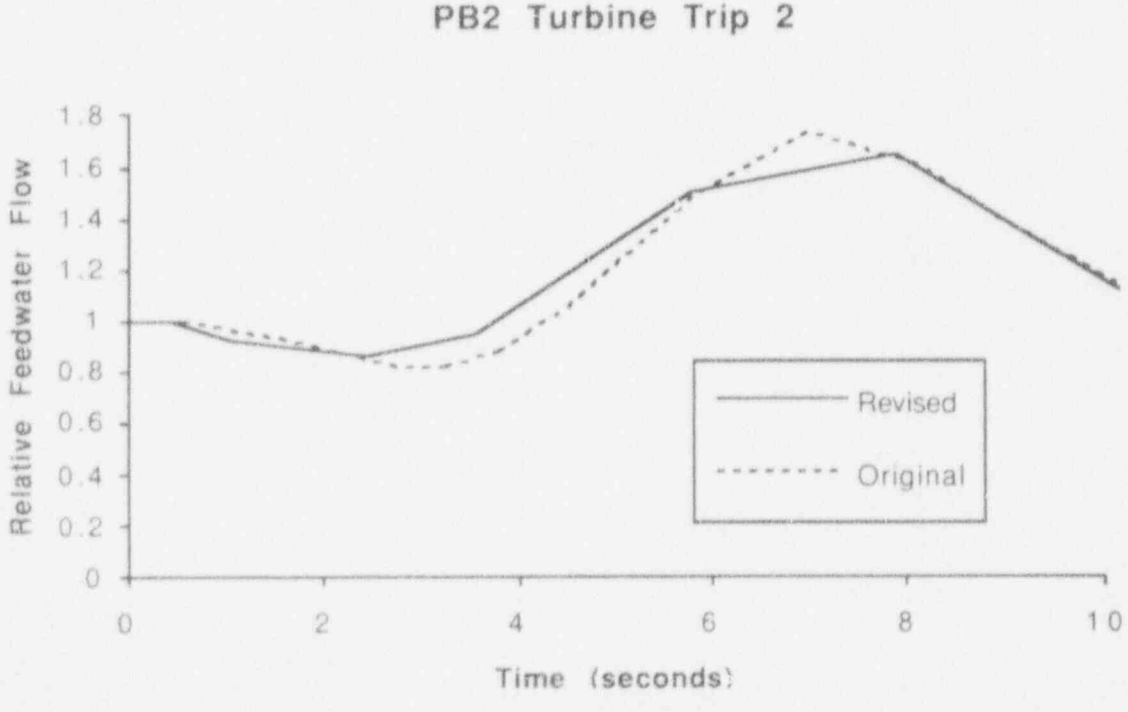


Figure 6-6 Comparison of Peach Bottom 2 TT2 Boundary Conditions

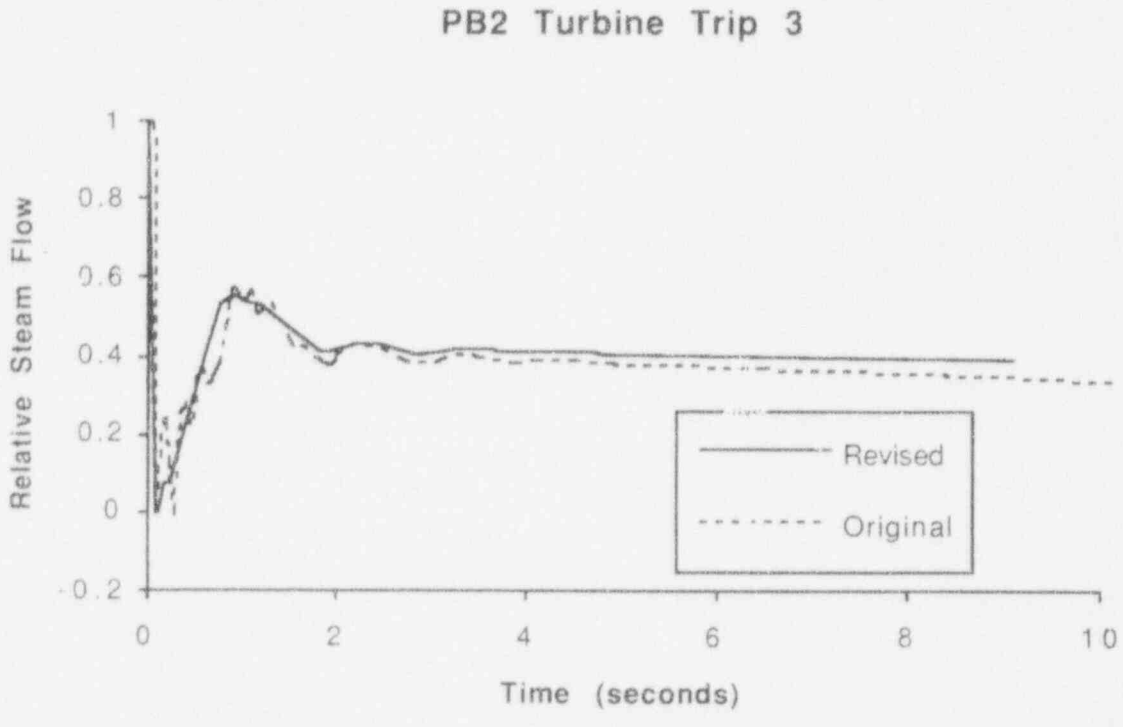


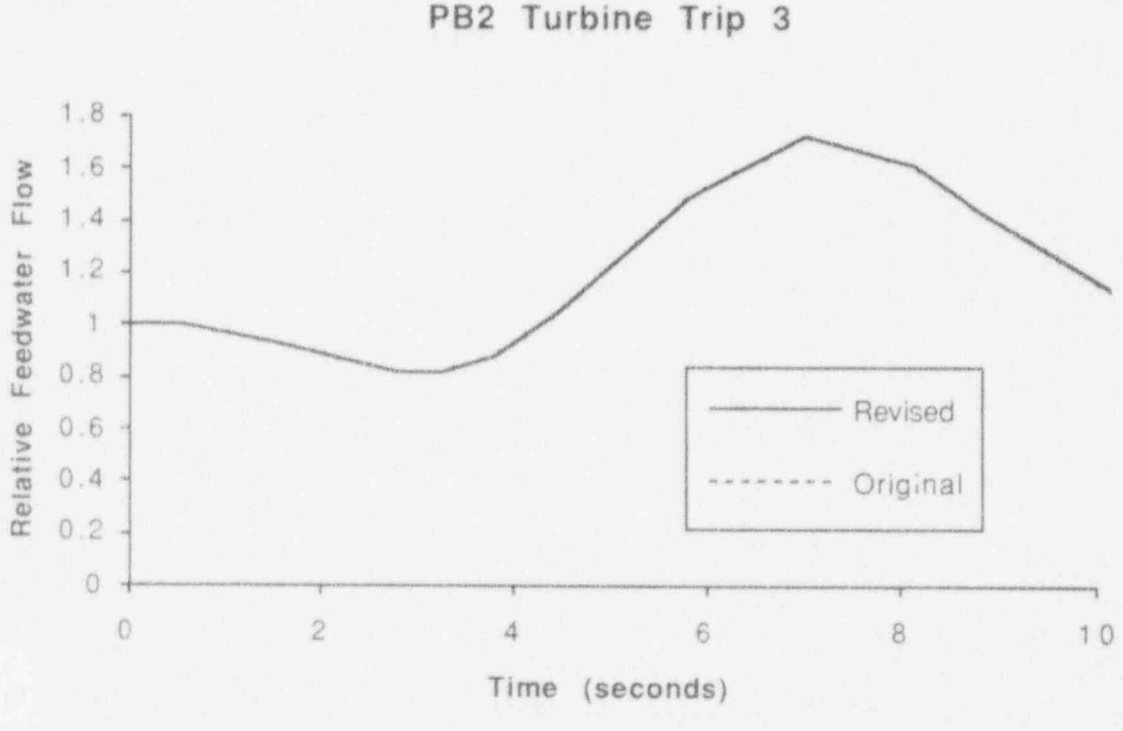


Figure 6-7 Comparison of Peach Bottom 2 TT3 Boundary Conditions

[Proprietary Information Deleted]

Figure 6-8a through 6-16c

## 7 REFERENCES

1. "BISON - A One Dimensional Dynamic Analysis Code for Boiling Water Reactors," ABB Report RPA-90-90-P-A (proprietary) RPA-90-90-NP-A (non-proprietary), December 1991.

2. "Reference Safety Report of Boiling Water Reactor Reload Fuel," ABB Report CENPD-300-P (proprietary), CENPD-300-NP (non-proprietary), October 1994.

3. "SVEA-96 Critical Power Experiments on a Full Scale 24-rod Sub-Bundle," ABB Report UR-89-210-P-A (Proprietary), UR-89-210-NP-A (non-proprietary), October 1993.

4. "Fuel Rod Design Methods for Boiling Water Reactors," ABB Report CENPD-285-P (proprietary) CENPD-285-NP (non-proprietary), May 1994.

5. "CONDOR: A Thermal-Hydraulic Performance Code for Boiling Water Reactors," ABB Report BR-91-255-P-A (proprietary), BR-91-266-NP-A (non-proprietary), May 1991.

6. "OF64 - Result of Void Measurement," ASEA-Atom Report FRIGG-PM-69, February 1970.

7. "OF64B - Results of Void Measurements," ASEA-Atom Report FRIGG -M-105.

8. W. Wulf, "Steamline Dynamics," Brookhaven National Lab. Report BNL-NUREG-51186, April 1980.

9. Letter W. J. Johnson (Westinghouse) from A. C. Thadini (NRC), "Acceptance for Referencing of Licensing Topical Report WCAP-11236 Regarding the Westinghouse Boiling Water Reactor Transient Analysis Code, "BISON"", October 24, 1989 (Westinghouse Report WCAP-11236 was reissued to the NRC as ABB Report RPA-90-90-P-A).

10. "ABB Atom Nuclear Design and Analysis Programs for BWRs: Programs Description and Qualification," ABB Report BR-91-402-P-A (proprietary), BR-91-403-NP-A (non-proprietary), May 1991.

## 8 NOMENCLATURE

A Cross section area of the flow channel [$m^2$]

D Hydraulic diameter [m]

I Moment of inertia [kg $m^2$]

L Cell length [m]

h Steam enthalpy per unit mass [J/kg]

P Steam pressure [Pa]

q Source term in energy equation [W/m]

Q Power output [W]

t Time [s]

v Steam specific volume [$m^3$/kg]

V Cell volume [$m^3$]

W Net mass flow rate [kg/s]

z Coordinate [m]

$\varepsilon$ Pipe wall roughness [m]

$\kappa$ Isentropic exponent [-]

$\lambda$ Darcy friction factor [-]

$\eta$ Efficiency [-]

$\rho$ Steam density [$kg/m^3$]

$\zeta$ Local loss of pressure coefficient [-]

$\theta$ integration factor

Subscripts and Superscripts

j Iteration level index

k Cell index

| | |
|---|---|
| k-, k+ | Left and right interface index respectively |
| n | Time level index |
| g | Generator |
| t | Turbine |
| s | Isentropic expansion |

ABB Combustion Engineering Nuclear Operations
Combustion Engineering, Inc.
1000 Prospect Hill Road
Post Office Box 500
Windsor, Connecticut 06095-0500
Telephone: (203) 285-9678
Fax: (203) 285-4117